We are IntechOpen,
the world's leading publisher of Open Access books
Built by scientists, for scientists

6,900
Open access books available

185,000
International authors and editors

200M
Downloads

154
Countries delivered to

Our authors are among the

TOP 1%
most cited scientists

12.2%
Contributors from top 500 universities

Interested in publishing with us?
Contact book.department@intechopen.com

Numbers displayed above are based on latest data collected.
For more information visit www.intechopen.com

Chapter

A Review on Metal Oxide-Graphene Derivative Nano-Composite Thin Film Gas Sensors

Arnab Hazra, Nagesh Samane and Sukumar Basu

Abstract

Most of the available commercial solid-state gas/vapor sensors are based on metal oxide semiconductors. Metal oxides (MOs) change their conductivity while exposed to gas or vapors ambient can be utilized as gas or vapor sensing materials. In recent days, graphene has attracted tremendous attention owing to its two-dimensional structure with an extremely high surface to volume ratio, electron mobility, and thermal conductivity. However, intrinsic graphene is relatively inefficient for the adsorption of gas/vapor molecules. In this regard, graphene oxide (GO) and reduced graphene oxide (rGO), which are graphene species functionalized with different oxygen groups that offer a higher amount of adsorption sites improving the sensitivity of the film. Up to now, many research groups across the globe have reported the promising performance towards gas detection using various GO/rGO-metal oxide nanocomposites. This chapter reviews the composites of graphene oxide or reduced graphene oxide and metal oxides in nanoscale dimensions (0-D, 1-D, 2-D, and 3-D) for gas sensing applications considering two specific focus areas, that is, synthesis of nanocomposites and performance assessment for gas/vapor sensing.

Keywords: nanoscale metal oxide, graphene derivatives, nanocomposites, efficient gas sensing

1. Introduction

In today's world, gas/vapor sensors have received significant attention because of their important applications in numerous areas such as environmental monitoring at industry and domestic area [1], disease diagnosis [2], agriculture [3], industrial wastes [4], food quality monitoring, etc. The detection of gases like NO, NO_2, NH_3, CO, CO_2, SO_2, H_2S, etc. is essential in many fields especially in environmental monitoring due to their toxicity and the related risk to the ecosystem [1–4]. Detection of volatile organic compounds (VOCs) is of great importance in environmental safety, supervision of human health, and food quality monitoring [1–3]. The detection of frequently used VOCs like acetone [5], formaldehyde [6], methanol [7], etc. is essential because they produce toxic effects, even in low concentrations, on human health. Detection of ethanol in human breath is important to restrict the

drunken driving-related issue [8]. Timely detection of released VOCs from stored vegetables and fruits is important to monitor their quality and freshness [9]. So, simple and reliable detections of gases and VOCs are important in everyday life.

Most of the existing commercial gas/vapor sensors are based on metal oxide (MO) semiconductors and polymer materials. However, the limitations of these gas sensors can be one or more as follows: costly, low sensitivity in lower ppm or ppb level, poor selectivity, limited lifetime, poor repeatability, difficult to miniaturization high power consumption [4, 10, 11], etc. As an alternative, nanostructured material-based gas/vapor sensors have gained significant importance due to many promising electrical, thermal, and optical characteristics combined with very high effective surface area, high sensitivity, fast response and recovery, selectivity, repeatability and stability [11], etc. Different carbon nanomaterials, such as graphene, graphene oxide (GO), carbon nanotube (CNT), charcoal, etc. have been shown to be promising gas/vapor sensing behavior due to the simple modifying their sensitivity by easy chemical treatments [12–14].

The limitations of intrinsic graphene are: (i) difficult to synthesize in large scale, (ii) it has almost no functional groups that can use for the adsorption of gas/vapor molecules, and (iii) it has metallic behavior with almost zero band gap [4, 13]. The prime performance enhancement methods in graphene-based sensors are found to be suitable impurity doping, composite formation, functionalization, implementation in field-effect transistor (FET) structure, etc. In this situation, reduced graphene oxide (rGO), which is graphene functionalized with different oxygen groups that provide enhanced adsorption sites, is more favorable for improving sensitivity. Besides very high thermal stability, the rGO sample contains many dangling bonds which can act as adsorption sites for gas analytes [15, 16].

Although many literatures suggested that the gas sensing performance can be improved by the structural and morphological variations, this is an insufficient approach for the growing demands of the gas/vapor sensing device performance. Single component transition metal oxide and carbon-based materials still suffer from some limitations arising from their inadequate physical and chemical characteristics that may hinder their large scale applications for high-performance gas/vapor sensors. Owing to their variable chemical conformation, synergistic properties, heterostructured nano-hybrids components, and nanocomposites are expected to show more admirable gas/vapor sensing performance [15, 17].

Metal oxide nanostructures are frequently hybridized with (i) noble and transition metals like Pd, Pt, Au, Ag, Ni, Nb, and so on, (ii) other metal oxides, (iii) carbon-based nanomaterials like CNT, graphene, and graphene-derivatives like GO and rGO to improve the gas sensing performance. Among all these functionalized materials, graphene and its derivatives attract tremendous attention for hybridizing with nanostructured metal oxides for promising gas/vapor sensing applications. Improvement of gas sensing properties of graphene/metal oxides hybrids principally depends on the following four factors:

(i) graphene derivative like GO or rGO supplies more dangling bonds and active interaction sites for gas/vapor molecule adsorption/reaction; (ii) its large effective surface area also enhance the gas sensing performance [15, 16]; (iii) metal oxide nanostructures have been extensively discovered as gas/vapor sensors due to the relatively high sensitivity of their electrical conductance to the target adsorbents. Thus the presence of rGO layers on metal oxide surface, electrical properties exhibit large and fast changes in the occurrence of gases/vapors improving overall sensing performance of the sensor; (iv) while GO and rGO show ambipolar behavior in the electron and hole concentration, they show hole-dominant p-type conducting properties owing to the adsorbed water and oxygen molecular species. Also, a nanocomposite of p-type rGO with an n-type transition metal oxide form a p-n

heterojunctions and the resulting complex nanostructure may exhibit better sensing performances than those of the individual materials. Numerous research has confirmed that the p-n heterojunction formed by p and n-type materials can play a positive role in the sensing mechanism [18–20].

However, a wide variety of nanostructured metal oxides and its composite with GO and rGO have been reported for efficient gas/vapor sensing applications in last one decade. In this chapter, we have categorized the graphene nanocomposites based on the morphology of metal oxides, that is, zero-dimensional (0-D like nanoparticles, quantum dots, etc.), one dimensional (1-D like nanorods, nanotubes, nanofibers, etc.), two dimensional (2-D like nanosheets, nanoplates, etc.), and three-dimensional (3-D like nanoflower, nanospheres, etc.). Synthesis, fabrication of graphene/nanoscale metal oxides nanocomposites and their performance assessment for gas/vapor sensing application are the main objective of the article.

2. Synthesis nanoscale metal oxides and graphene derivatives composite

In this section, the synthesis of graphene and its derivatives like graphene oxide (GO) and reduced graphene oxides (rGO) is described in the first sub-section. Then the synthesis of nanoscale metal oxides, as well as the nanohybrid formation, is described in the next sub-section.

2.1 Synthesis of graphene and graphene-derivatives

Graphene is considered as the parent of all graphitic forms [21]. The purest form of graphene is named as pristine graphene (with no heteroatomic contamination) where 'scotch tape method' widely accepted for producing the highest quality of graphene [22]. Graphene produced from micromechanical cleavage, that is, adhesive tape method can isolate only a small amount of graphene, hence this method is used to isolate graphene for research purposes. For large scale production of graphene, various methods have been reported in the literature which can be broadly classified into two categories: top-bottom approach and bottom-up approach [23].

Top-bottom methods mainly involve breaking of the van der Waals bonds which hold layers of graphene to form graphite [22]. Top-bottom approach involves electrochemical exfoliation, exfoliation of graphite intercalation compounds (GIC), micromechanical cleavage, solvent-based exfoliation of graphite oxide, arc discharge, etc. [23]. Among these methods, exfoliation of graphite oxide has received great attention as graphite oxide is easily produced by oxidation of graphite as reported in the Hummers method. Graphite oxide is exfoliated to obtain graphene oxide which is reduced to form reduced graphene oxide (rGO). Reduction process can be thermal, chemical, or UV-based method [24]. Bottom-up approach involves forming of large-area graphene sheet via growth over the substrates and one of the most potential methods is chemical vapor deposition (CVD) [23].

Along with graphene, researchers have also worked on the synthesis of graphene oxide (GO) as well as reduced graphene oxide (rGO) in recent years. rGO nanoparticles was prepared by thermal reduction of GO which is again obtained from Hummer's method [25]. However, the required quality of graphene and graphene derivatives (rGO, GO) depends on its applications and based on that the methods of production are decided. Till date, CVD [26, 27] and modified Hummer's method [28–30] are most suitable for the synthesis of graphene and GO, respectively, in context of the formation of metal oxide/graphene, metal oxide/rGO, metal oxide/GO nanocomposite.

2.2 Synthesis metal oxide nanostructures and graphene derivatives composites

Synthesis of hybrid graphene with different nanoscale metal oxides are classified in four categories, that is, graphene/0-D metal oxides, graphene/1-D metal oxides, graphene/2-D metal oxides, and graphene/3-D metal oxides.

2.2.1 Synthesis of graphene/0-D metal oxides composites

Synthesis of metal oxide nanoparticles (NPs) and GO/rGO composites which was used for efficient gas sensing applications is described in this section. Among all the metal oxides, SnO_2 was reported mostly to synthesize nano composites with graphene and its derivatives (GO and rGO). At the same time, nanoparticles of metal oxides were preferred majorly to prepare the monohybrids with GO and rGO. Different chemical synthesis techniques were followed to develop the nanocomposites of metal oxide/rGO like hydrothermal, solvothermal, flame spray pyrolysis, etc. [31, 32].

Hydrothermal is one of the commonly reported techniques for preparing metal oxide nanoparticles-rGO composites. Among different metal oxides, SnO_2 nanoparticles were reported extensively to prepare nano-hybrid with rGO for efficient gas sensing application [33–42]. SnO_2/rGO [33–35] nano-hybrid was prepared by facile hydrothermal treatment where precursor was prepared with mixture of $SnCl_4$, HCl, H_2O, and GO (or rGO). Heating temperatures were reported as 120°C [33] and 180°C [34, 35] whereas the heating time was 12 h, consistent for all the reports. Different weight% (0.5–5 wt.%) of Au was added in the SnO_2/rGO nanocomposite by using $HAuCl_4$ salt to study the effect of Au concentration on the sensitivity of SnO_2/rGO gas sensors [34]. Scanning electron micrograph (SEM) of SnO_2/rGO films which was used for promising gas sensing application are represented in **Figure 1(a** and **b)**. Mishra et al. reported rGO/SnO_2 nanocomposite by surfactant-assisted hydrothermal method, in which hexamethyldisilazane (HDMS) was used as a surfactant [36]. Ghosh et al. [37] reported SnO_2 nanoparticle synthesis by hydrothermal method and SnO_2/rGO film synthesis by mixing of SnO_2 nanoparticles with GO. The GO-SnO_2 mixture was then ultrasonicated to obtain uniform dispersion. Then the sample was drop cast on the platinum electrode and heated at 160°C to reduce GO and get SnO_2/rGO hybrid sensing layer [37]. The hydrothermal method was also used for the synthesis of SnO_2/rGO hybrid with
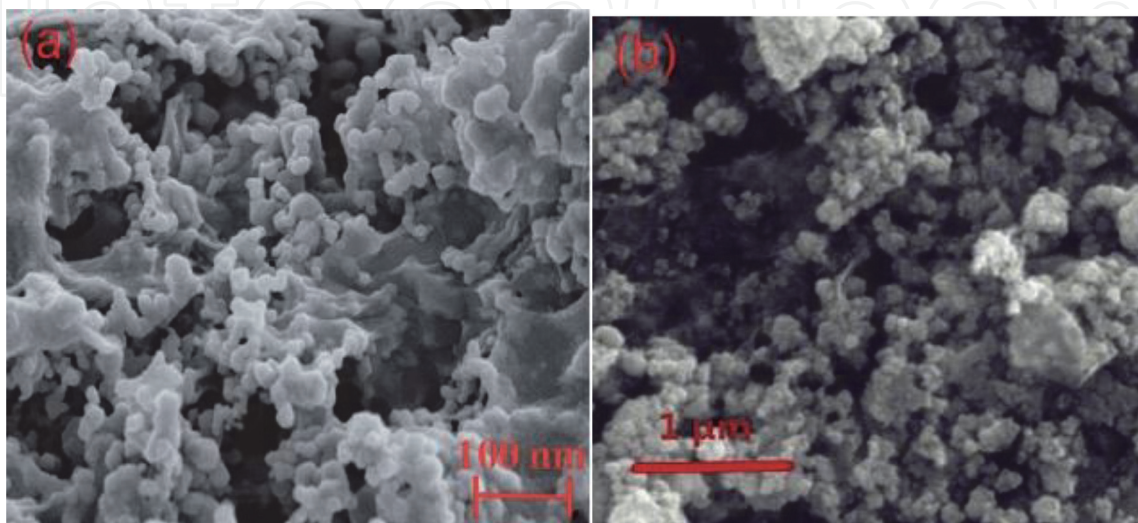

Figure 1.
SEM image of hydrothermally grown SnO_2 nanoparticles and rGO composites reported by (a) Zhang et al. [33] and (b) Peng et al. [41].

a high concentration of oxygen vacancy [40, 42] and Pt-activated SnO_2 nanoparticles-rGO hybrid [41]. Transmission electron micrograph (TEMs) of SnO_2 quantum dot decorated on rGO surface is represented in **Figure 2(a–c)**.

NiO/rGO nanohybrid [39] was prepared via two-step hydrothermal treatment. NiO nanoparticles powder was prepared by hydrothermal method using $NiCl_4 \cdot 6H_2O$ as the source of Ni and then calcined at 400°C. NiO nanoparticle powder was then mixed with rGO solution and treated by hydrothermal method with a various ratio of NiO/rGO as 2:1, 4:1, and 8:1 (**Figure 3**).

Undoped and Ni-doped SnO_2 nanoparticle and graphene composites were developed by flame spray pyrolysis (FSP) method as reported in references [32, 43], respectively. About 0.1–2 wt.% Ni-doped SnO_2 nanoparticles were synthesized by FSP technique and graphene was produced from graphite by the electolytic exfoliation technique. Then, a paste was prepared by mixing Ni-doped SnO_2 and graphene powder and finally spin coating method was used to deposit a film for gas sensing application. Bright field (BF) TEM images of 0.5 wt.% SnO_2 NPs loaded graphene composites and 2 wt.% Ni doped SnO2 NPs loaded graphene composites are represented in **Figure 4(a)** and **(b)**, respectively.

ZnO/rGO composite was prepared by the solvothermal method for low-temperature acetylene sensing as reported by Iftekhar Uddin et al. [44, 45]. ZnO powder was prepared through the solvothermal method by using $Zn(NO_3)_2$ and NaOH in ethanol at 120°C. Ag-loaded ZnO/GO hybrid was synthesized by chemical route. $AgNO_3$ was added to the ZnO/GO solution with 2:1 ratio, then stirred continuously for 30 min. Hydrazine hydrate was then added to the mixer to reduce GO
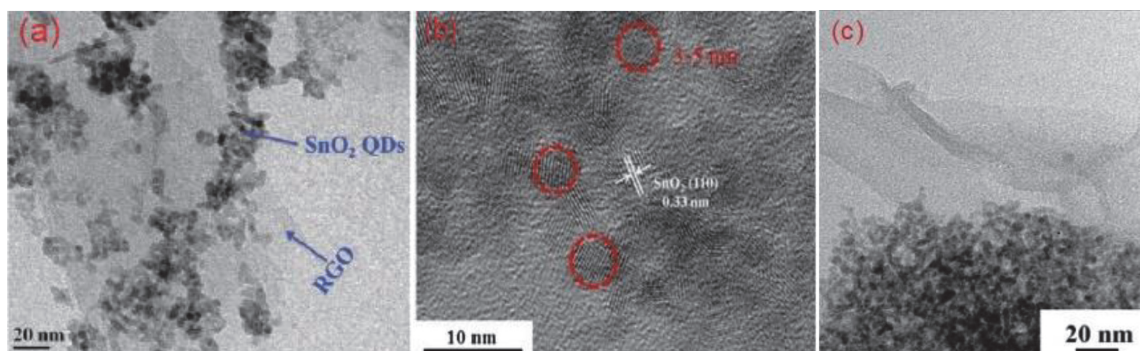

Figure 2.
TEM images of hydrothermally grown SnO_2 nanoparticles and rGO composites (a) SnO_2 quantum dot on rGO film surface [36], (b) high resolution (HR) TEM image of SnO_2 NPs on rGO [40], and (c) dense SnO_2 NPs on rGO [42].
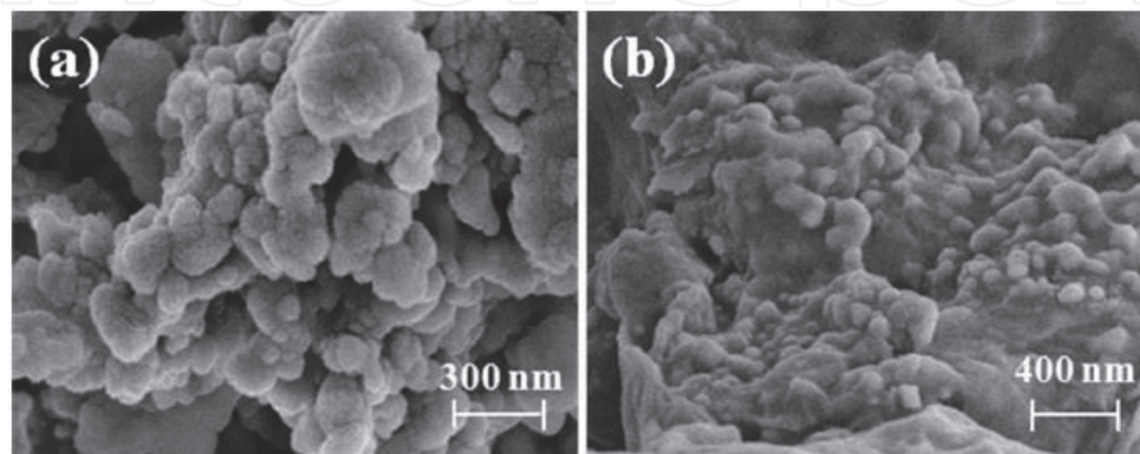

Figure 3.
SEM of hydrothermally grown (a) NiO NPs and (b) NiO/rGO nanocomposites with 2:1 ratio [39].
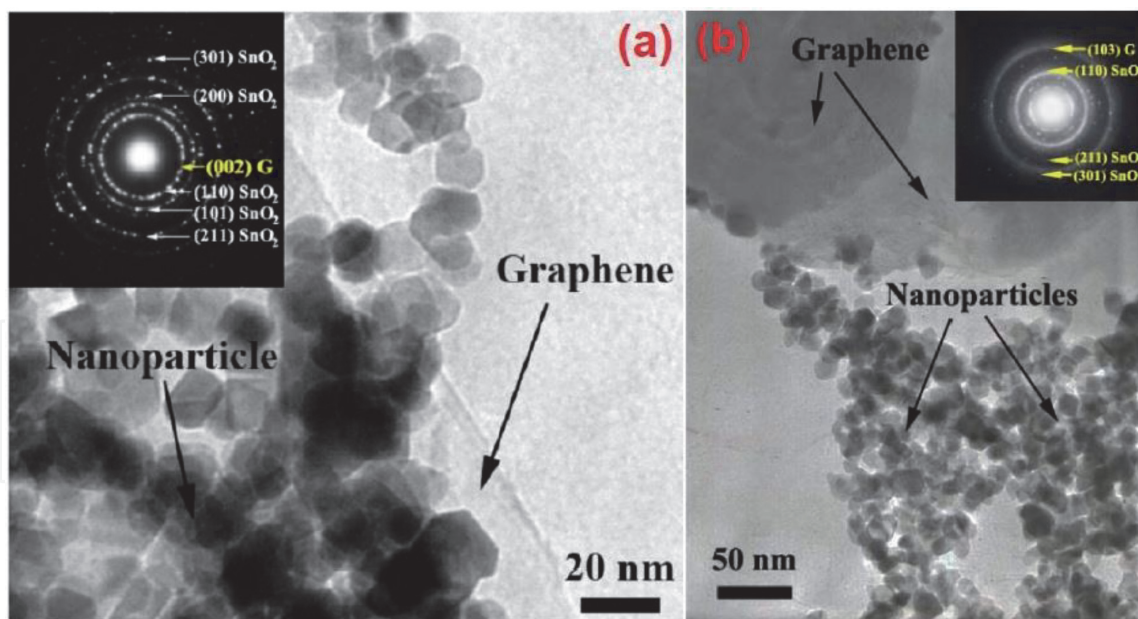
Figure 4.
BF TEM images of 0.5 wt.% SnO₂ NPs loaded graphene composites and 2 wt.% Ni-doped SnO₂ NPs loaded graphene composites. Inset: Corresponding selected area electron diffraction (SAED) pattern [32, 43].
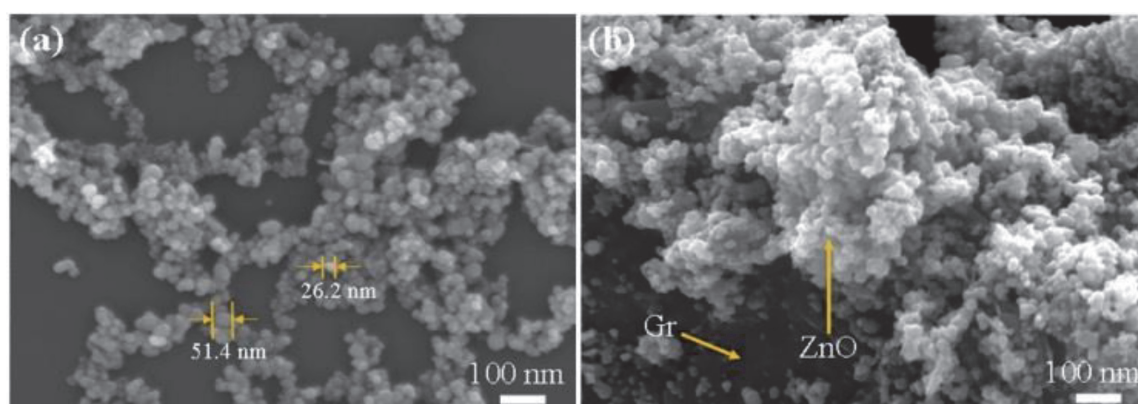

Figure 5.
Plane-view FESEM micrographs of (a) pure ZnO nanoparticles and (b) ZnO nanoparticle rGO hybrids [44].

at 110°C for 8 h [44]. Morphology of ZnO NPs and rGO nanocomposite is shown in **Figure 5(a** and **b)**.

ZnO quantum dots (QDs) decorated on graphene nanosheets were synthesized by facile solution-processed method (**Figure 6(a)**). ZnO QDs were nucleated and grown on the surface of graphene by controlling the distribution density by reaction time and precursor concentration [46]. ZnO-rGO hybrid was prepared by wet chemical method followed by deposition of Au using HAuCl4, which was added to the ZnO-rGO dispersion. Finally, the addition of NaBH₄ through sonication process completed the formation of ZnO QD [47]. To understand the impact of particle size on gas sensing performance, Tung et al. [48] prepared rGO-Fe₃O₄ nanoparticle hybrid with different particle sizes (5, 10, and 20 nm) via in situ chemical reduction of GO in presence of poly-ionic liquid (PIL) (**Figure 6(b)**). Kamal [49] prepared graphene-NiO nanoparticles composites by decomposition of nickel benzoate dihydrazinate complex used for hydrogen sensing application.

Graphene oxide was synthesized from natural graphite flakes by Hummers' method which was further used to prepare rGO-CuFe₂O₄ nanocomposite by combustion method [50]. In this process, sonicated GO was dissolved with 1:2 ratio of
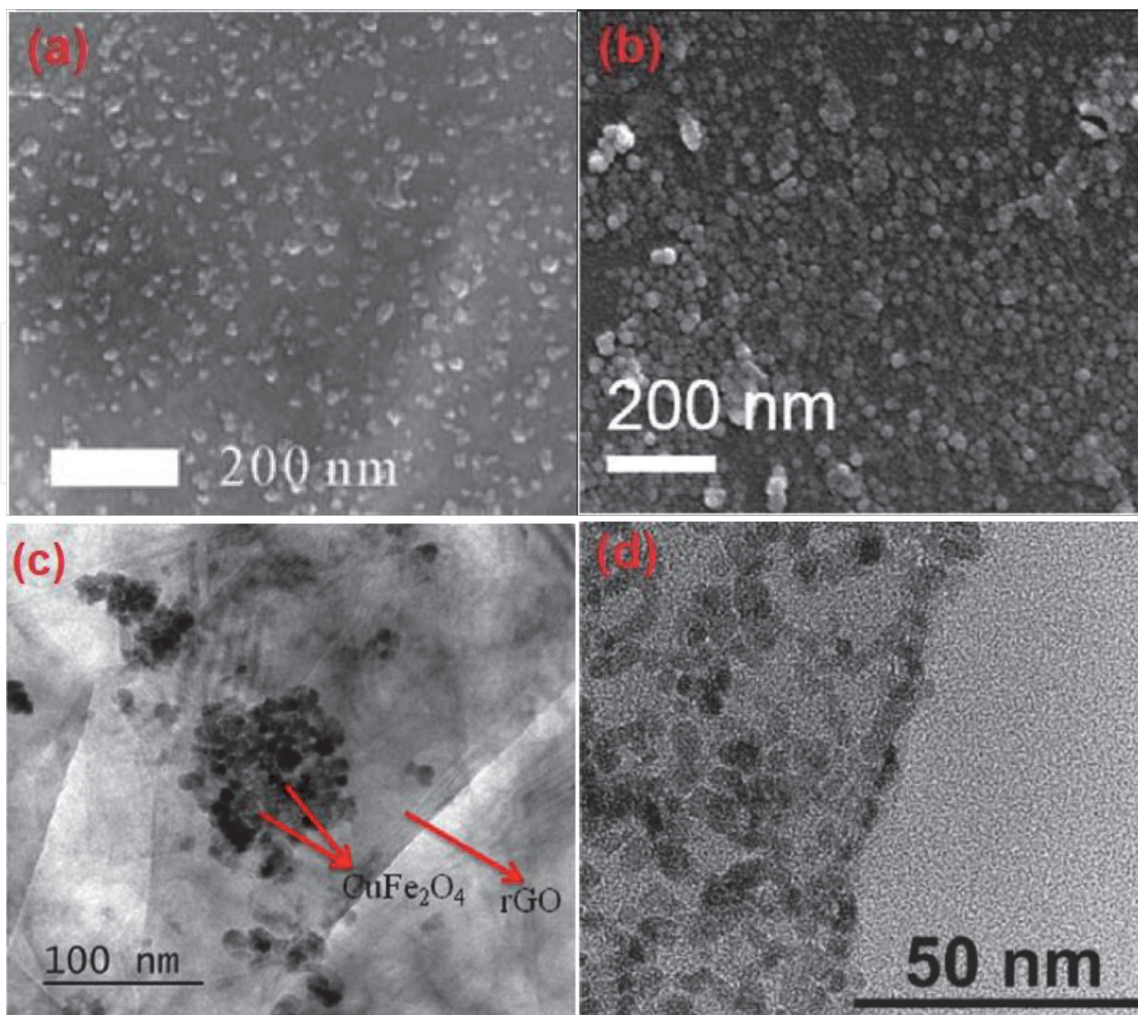
Figure 6.
SEM images of (a) ZnO QDs/graphene nanocomposites [46], (b) rGO-Fe₃O₄ nanoparticles [48] synthesized by facile solution-processed method. TEM images of (c) rGO-CuFe₂O₄ by combustion method [50] and (d) microwave assisted rGO-SnO₂ nanparticles composites [51].

Cu^{2+} to Fe^{3+} salts and distilled water. The resulting mixture was stirred at 100°C to get a viscous solution which was further heated around 450°C in a muffle furnace. Finally, the mixture was frothed and it gave a foamy powder of nanocomposite (**Figure 6(c)**). The one-pot microwave-assisted non-aqueous sol-gel method was used to synthesize pure SnO_2 nanoparticles and SnO_2/rGO nanocomposite (**Figure 6(d)**) [51]. Kim et al. [52] reported the microwave-assisted the formation of SnO_2/graphene nanocomposite in which mixture of SnO_2 nanopowder and graphene flakes dispersed in ethanol, the resulting solution was dried. The dried powder mixture was treated in the commercial microwave heater for heating process. Microwave-treated powder was again dispersed in ethanol and then the solution was spray-coated on SiO_2 substrate placed on a hot plate. Along with SnO_2/graphene nanocomposite, a small amount of secondary SnO_x (x < 2) nanoparticles were also deposited on the surface. Secondary SnO_x nanoparticles tend to increase as the microwave heating time is increased [52].

2.2.2 Synthesis of graphene/1-D metal oxides composites

One dimensional (1-D) nanostructures of the metal oxide like nanotubes, nanorods, nanofibers, nanowires, etc. are considered as most promising for the detection of analytes in gaseous phases [53, 54]. Owing to its large surface-to-volume ratio, large open porosity and most importantly one of its dimension is

comparable to the Debye length which enhances the gas sensitivity significantly. Gas sensing performance is improved further in 1-D materials by using as a nanocomposite with graphene, GO and rGO. Here, we reviewed different methods used for the synthesis of 1-D metal oxide nanostructure and its composite with graphene and graphene derivatives.

ZnO nanowires (NW) and graphene hybrid architecture were reported by Yi et al. [55] where graphene sheets covered with thin metal layers were used as top electrodes for ZnO where graphene sheets coated with thin metal layers were employed as top electrodes for ZnO vertical-NW channels. The ZnO NWs-graphene/metal hybrid architectures maintained sufficient spaces between the NWs for easy and fast gas transport. However, ZnO nanorods (NRs) were synthesized by using hydrothermal reaction and graphene sheets were synthesized by the CVD method and transferred to the top of the ZnO NRs by PMMA treatment. The scanning electron micrograph of ZnO NRs-graphene/metal hybrid architectures are represented in **Figure 7(a)**. Single crystalline WO_3 nanorods on the surface of graphene were synthesized through a one-step hydrothermal method [56]. WO_3 nanorods with 3.5 wt.% graphene composites improved gas sensitivity of 25 times showing good selectivity towards NO_2. SEM image of WO_3 nanorods and graphene hybrids is shown in **Figure 7(b)**.

Large-scale sandwich-like heterostructures of ZnO nanorod arrays with reduced graphene oxide sheets were reported by Zou et al. [30] as shown in **Figure 7(c)**. Highly dense ZnO nanorods were grown by hydrothermal method and double sides coverage of reduced graphene sheets by ZnO NRs formed a sandwich like heterostructures of ZnO/graphene/ZnO for efficient ethanol detection.

Electrospinning is a potential and well-reported technique for the synthesis of nanofibers (NFs) network of metal oxides. N,N-dimethylformamide (DMF) and polyvinyl pyrrolidone (PVP) are mixed with target metal oxide precursor and the whole mixture is poured into a syringe having a suitable needle attached. A high voltage (a few kV, DC) is applied between the needle and the collector plate to get the NFs of the target metal oxides. In electrospinning method, composites of metal oxide NFs and graphene derivatives are synthesized by two different routes, that is, (i) GO or rGO solutions are added into the base mixture before electrospinning and (ii) synthesized NFs are decorated with GO or rGO solutions. rGO/Co_3O_4 NFs [57] and rGO/ZnONFs composites [54] were synthesized where rGO was added into the precursor before electrospinning and both the nanohybrids were tested towards different gases and vapors like NH_3, ethanol, etc. rGO/Co_3O_4 NFs [58], rGO/SnO_2 NFs [53], and rGO/WO_3 NFs composites [59] were synthesized where Co_3O_4, SnO_2, and WO_3 nanofibers were synthesized by electrospinning method first and then functionalized with rGO solution. All three composites were used to detect acetone in the selective route. **Figure 8(a)** and **(b)** represents the TEM and SEM images of
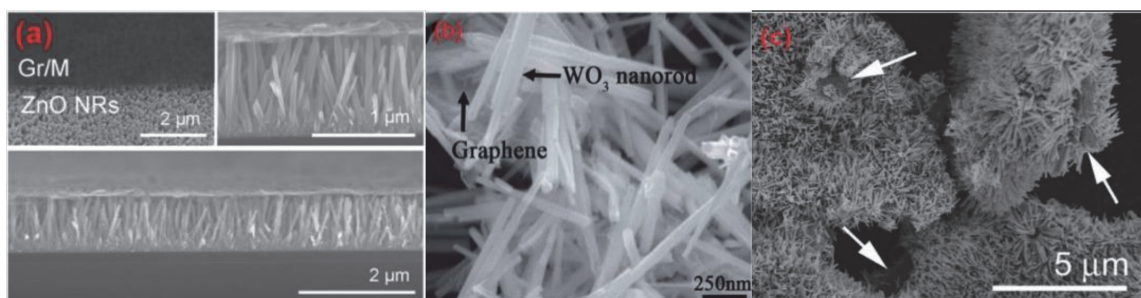

Figure 7.
SEM images of 1-D metal oxides and graphene nanocomposites synthesized by hydrothermal route (a) ZnO NRs-Gr/M hybrid architectures [55], (b) WO_3 nanorods/graphene composites [56], and (c) ZnO/G array structures [30].
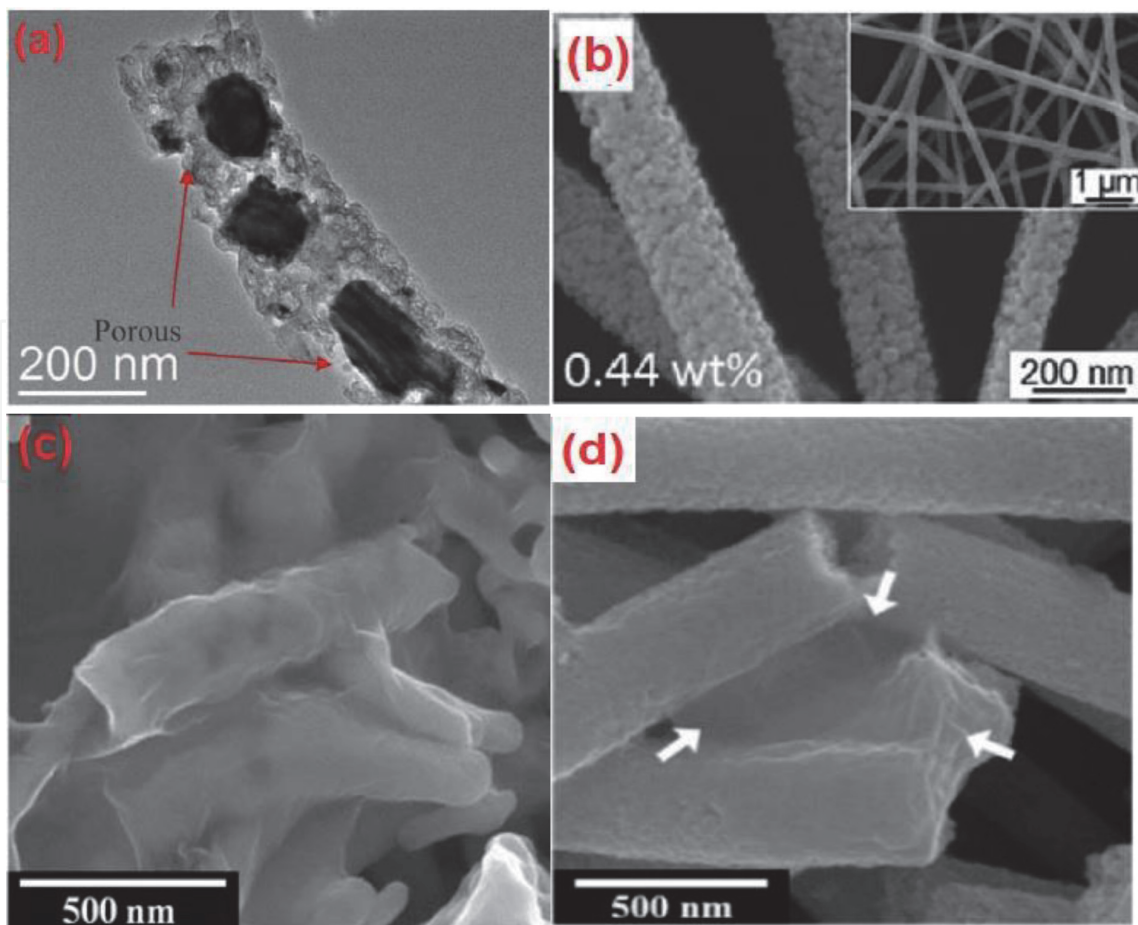
Figure 8.
(a) TEM images of rGO/Co$_3$O$_4$ NFs [57], (b) SEM image of rGO/ZnO NFs composite [54], SEM image of (c) rGO/Co$_3$O$_4$ NFs composites [58], and (d) rGO/SnO$_2$ NFs composites [53].

rGO/Co$_3$O$_4$ NFs [57] and rGO/ZnONFs composite [54], respectively. Here, rGO film was almost invisible due to the mixing of rGO in solution before electrospinning. rGO film was clearly visible in rGO/Co$_3$O$_4$ NFs [58] and rGO/SnO$_2$ NFs [53] composites in SEM images shown in **Figure 8(c)** and **(d)** as the rGO functionalization was carried out after electrospinning.

Synthesis of TiO$_2$ nanotubes array was done by electrochemical anodization of metallic titanium films [60] and rGO/TiO$_2$ nanotubes composite was synthesized by electrodeposition of rGO on TiO$_2$ nanotubes [61, 62]. Electrodeposition method was also used to synthesize ZnO nanorods and selective electrochemical etching of those nanorods to synthesized ZnO nanotubes. rGO/ZnO nanotubes hybrid structure was synthesized by dip-coating technique for efficient alcohol sensing application [63].

One step colloidal synthesis was employed for rGO/SnO$_2$ quantum wire nanocomposite for room temperature H$_2$S sensing [25]. Single crystal SnO$_2$ nanowire was directly grown on the platinum electrode by thermal evaporation and composites was formed by using CVD grown graphene layer for efficient NO$_2$ sensing [26]. Hydrolysis method was used in absence as well as in presence of GO to form ZnO nano-seed and GO supported ZnO nano-seed, respectively, and ultrathin ZnO nanorod/rGO mesoporous nanocomposites were synthesized for NO$_2$ sensing [29].

2.2.3 Synthesis of graphene/2-D metal oxides composites

Metal oxides nano-sheets and nameplates were functionalized with graphene and its derivatives for efficient gas sensing behavior. Ni-doped ZnO nanosheets

were deposited on a p-Si substrate by using radio frequency (RF) sputtering techniques. GO was synthesized by Hummer's method and reduced thermally at high temperature (600°C). rGO flakes were then decorated on Ni-doped ZnO nanosheets by drop-casting method. rGO/Ni-doped ZnO nanosheets were used for low ppm hydrogen detection [64]. Highly wrinkled SnO_2/rGO composite was synthesized by one-time hydrothermal technique and used for the detection of ethanol at 250°C (**Figure 9(a)**) [65]. Nanocomposites of ZnO nanosheets and GO were synthesized for highly efficient acetone sensing. The nanocomposites sensor was flexible, high effective surface area and enhanced functional groups due to GO which were in favor of gas adsorption (**Figure 9(b)**) [66]. rGO/hexagonal WO_3 nanosheets hybrid materials were fabricated through the hydrothermal method and post-annealing treatment. 2-D porous WO_3 nanosheets were attached on rGO. The sensor based on 3.8 wt.% rGO/hexagonal-WO_3 composites offered promising sensing performance to H_2S [67].

2.2.4 Synthesis of graphene/3-D metal oxides composites

3-D metal oxides like nanoflower and nanosphere were used to synthesize nanocomposites with graphene and its derivatives by the hydrothermal and sol-gel method [15, 68–70].

Hybrids with flower-like hierarchical ZnO and rGO were synthesized by the facile and mild solution-processed method. Compared with the pristine flower-like ZnO, NO_2 sensing was increased significantly in case of hierarchical rGO/ZnO hybrids [15]. A facile one-pot hydrothermal method was used to synthesize rGO/In_2O_3 composites. The flower-like hierarchical structure of In_2O_3 showed high effective surface area enhancing the active interaction sites. In the composite, rGO formed local p-n heterojunctions enhancing the gas sensing performance significantly. The rGO/In_2O_3 composite exhibited an excellent selectivity towards NO_2 in the wide concentration range from 10 ppb to 1 ppm [68]. α-Fe_2O_3/rGO nanocomposites with nanosphere-like α-Fe_2O_3 structure were synthesized by a hydrothermal route at 120°C. α-Fe_2O_3 nanosphere was 40–50 nm in diameter and constructed by a few nanometer-sized nanoparticles where rGO was intercalated single sheets. These nanocomposites showed excellent response and selectivity towards NO_2 at room temperature [69]. Graphene-WO_3 nanostructure with
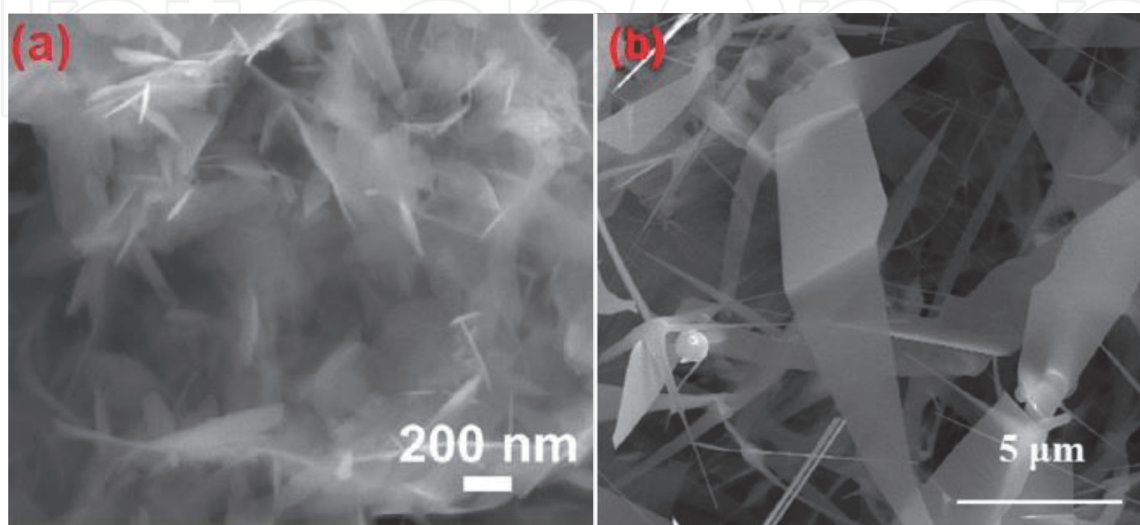

Figure 9.
SEM images of rGO/2-D metal oxide nanocomposites (a) wrinkled SnO_2/rGO composite [65] and (b) GO/ZnO nano-sheets [66].
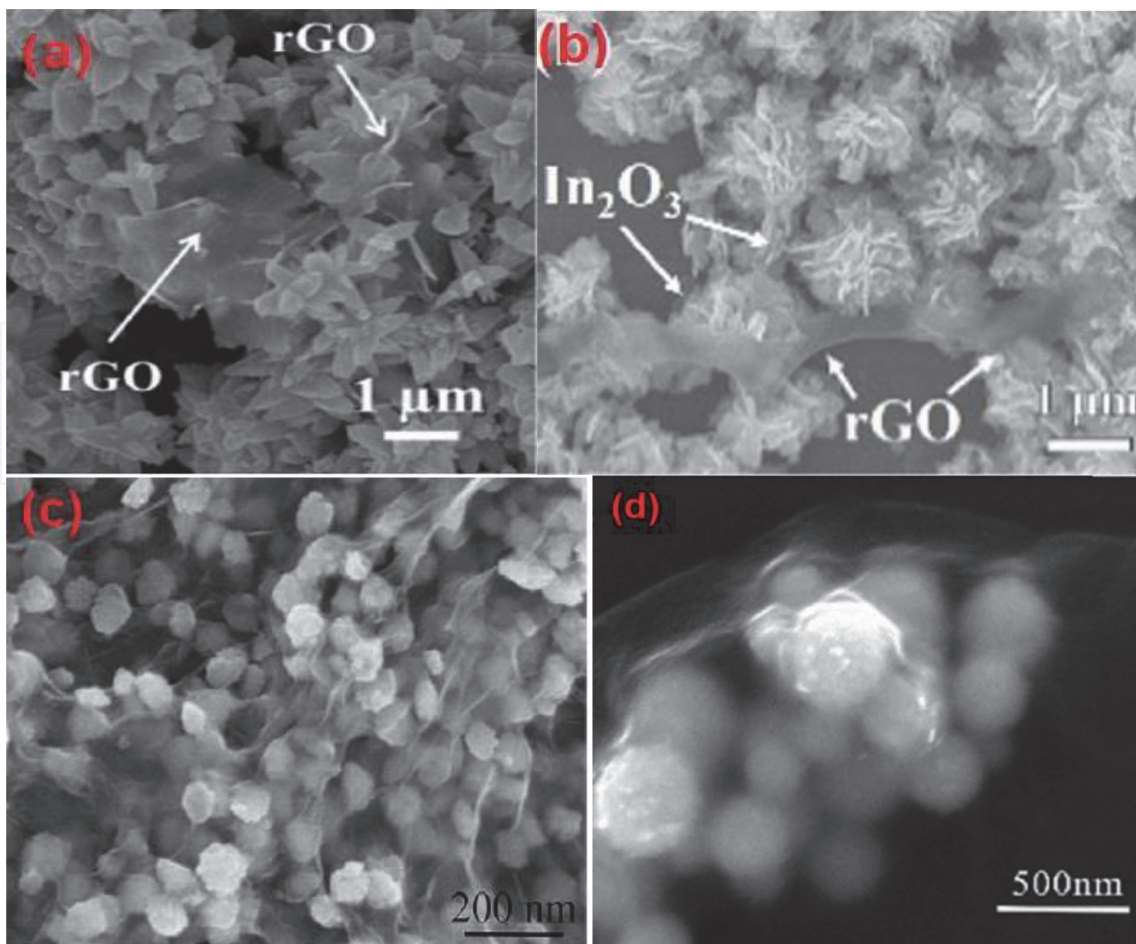
Figure 10.
SEM images of (a) rGO/flower-like hierarchical ZnO composites [15], (b) rGO/In₂O₃ nanoflower composite [68], (c) rGO/α-Fe₂O₃ nanosphere [69], and (d) graphene-wrapped WO₃ nanosphere [70].

gauze-like graphene nanosheets wrapping up spherical WO_3 nanoparticles was synthesized by a facile sol-gel method. Graphene-wrapped WO_3 nanocomposites offered uniform nanospheres with 200–400 nm diameter. Graphene/WO_3 nano-composites showed good sensitivity and selectivity to low concentrations of NO_2 gas at room temperature when pure WO_3 and graphene-based sensors did not show any response towards NO_2 at room temperature [70]. Scanning electron micrograph of 3-D metal oxides and graphene nanocomposites is shown in **Figure 10(a–d)**.

3. Assessments of gas/vapor sensing performances

3.1 Sensing performance of graphene/0-D metal oxides composites

Gas/vapor sensing performance of metal oxide nanoparticles (0-D) functionalized with graphene or graphene derivatives (GO, rGO) is represented in **Table 1** where 37 references are considered for performance assessment of graphene/0-D metal oxide oxides composites sensors.

Graphene/metal oxide NPs (0-D) composites and its gas sensing performance were explored extensively in case of SnO_2 where hydrothermal method was commonly used as the synthesis technique. The gas sensing performance of rGO/SnO_2 NPs was further improved by functionalization with Pd, Au, Pt, and Ag nanoparticles [31, 34, 41, 78]. ZnO nanoparticles occupied the second position to use as a nanocomposite with graphene and its derivatives other metal oxide

Composite material	Target gas/ vapor	Operating temperature (range) (°C)	Concentration and range (ppm)	Response magnitude	Response/ recovery time (s)	Ref.
Graphene-SnO_2 nanoparticles	NO_2	150 (30–190)	5 (1–5)	$R_{gas}/R_{air} = 72.6$	129/107	[52]
rGO/SnO_2 nanoparticles	Acetone	Room temperature	2000 (10–2000)	$R_{air} - R_{gas}/R_{air} = 9.72\%$	95/141	[33]
Graphene aerogel-SnO_2 nanoparticle	NO_2	Room temperature	200 (10–200)	$R_{gas} - R_{air}/R_{air} = -12\%$	190/224	[71]
Graphene-SnO_2 nanoparticles	H_2	50	100 (1–100)	$I_{gas}/I_{air} = 6$	1.1/1.1	[72]
rGO-SnO_2 quantum dots	H_2	200	500	$R_{air} - R_{gas}/R_{air} = 89.3\%$	~50/~155	[36]
	LPG	250	500	$R_{air} - R_{gas}/R_{air} = 92.4\%$	~80/~155	
rGO/SnO_2 nanoparticles	NH_3	200 (100–200)	1000 (25–2800)	—	—	[37]
rGO/SnO_2 nanoparticles	C_2H_2	180 (100–300)	50 (0.5–500)	$R_{air}/R_{gas} = 12.4$	54/23	[38]
rGO-SnO_2 nanoparticles	NO_2	30 (30–100)	1 (0.05–2)	$R_{air}/R_{gas} = 3.8$	14/190	[40]
rGO-SnO_2 nanoparticles	NO_2	Room temperature	5 (1–20)	$I_{air} - I_{gas}/I_{air} = 65.5\%$	12/17	[42]
Graphene/SnO_2 nanoparticles	NO_2	150 (25–350)	5	$R_{gas}/R_{air} = 26342$	13/—	[43]
rGO/SnO_2 nanoparticles	NO_2	50 (30–60)	5 (0.5–500)	$R_{air}/R_{gas} = 3.31$ (25% RH)	135/200	[35]
rGO/SnO_2 nanoparticles	SO_2	60 (22–220)	500 (10–500)	$R_{air} - R_{gas}/R_{gas} = {\sim}22$	144/210	[73]
Graphene/SnO_2 nanoparticles	NO_2	Room temperature	100 (0.3–100)	$G_g - G_o/G_o = {\sim}11$	—	[74]
Graphene/SnO_2 nanoparticles	Ethanol	350 (150–350)	1000 (50–1000)	965	1.8/~120	[76]
Graphene/SnO_2 nanoparticles	NO_2	60 (25–120)	4 (1–4)	$R_g - R_a/R_a = {\sim}22$	—	[75]
rGO/SnO_2 nanoparticles	CO	Room temperature	1600 (50–1600)	$R_g - R_a/R_a = 9.5\%$	~60/~60	[76]
Sulfonated graphene/SnO_2 nanoparticles	NO_2	Room temperature	5 (1–50)	$R_{air} - R_{gas}/R_{gas} = 1.203$	40/357	[77]
Graphene-SnO_2 nanoparticle with doped Ni	Acetone	350 (150–350)	200 (1–50)	$R_{air}/R_{gas} = 169.7$	5.4/150	[32]
Graphene-Pd/SnO_2 nanoparticles	H_2 Ethanol	Room temperature	20,000 200 (25–200)	$R_o - R_{gas}/R_o = 11\% (H_2), 14.8\%$ (ethanol)	34/27	[31]
rGO/SnO_2 nanoparticles decorated Au NPs	NO_2	50 (30–60)	50 (5–100)	$R_{gas}/R_{air} = 2.68$	19/20	[34]

Composite material	Target gas/vapor	Operating temperature (range) (°C)	Concentration and range (ppm)	Response magnitude	Response/recovery time (s)	Ref.
rGO-SnO$_2$ nanoparticles (activated by Pt)	Methanol	110 (20–180)	500 (10–500)	R_{air}/R_{gas} = 203	6/21	[41]
rGO/SnO$_2$ nanoparticles (with Ag NPs)	NO$_2$	Room temperature	5 (0.5–500)	R_{air}/R_{gas} = 2.17 (25% RH)	49/339	[78]
Graphene-ZnO quantum dots	HCHO	Room temperature	100 (25–100)	$G_g - G_o/G_o$ = 1.1	30/40	[46]
Graphene/ZnO nanoparticles	C$_2$H$_2$	250 (25–350)	100 (30–1000)	R_{air}/R_{gas} = 143	100/24	[45]
rGO/ZnO nanoparticles	NO$_2$	50 (25–140)	50 (5–275)	$R_g - R_a/R_a$ = 32%	96/1552	[74]
rGO/ZnO nanoparticles	NO$_2$	Room temperature	5 (1–25)	$R_g - R_a/R_a$ = 25.6%	165/499	[80]
3-D rGO/ZnO nanoparticle	CO	200	1000 (1–1000)	$R_g - R_a/R_a$ = 85.2%	7/9	[81]
rGO-ZnO/Ag nanoparticles	C$_2$H$_2$	150 (25–250)	100 (1–1000)	R_{air}/R_{gas} =21.2	25/80	[44]
rGO/ZnO-Au nanoparticles	NO$_2$	80 (60–90)	100 (20–100)	$R_{air} - R_{gas}/R_{air}$ = 32.55	27/86	[47]
Graphene-NiO nanoparticles	H$_2$	250 (100–350)	2000 (400–2000)	$R_g - R_a/R_a$ = 52.4%	NA	[49]
rGO/NiO nanoparticles	CH$_4$	260 (20–400)	1000 (100–1000)	$R_{air} - R_{gas}/R_{gas}$ = 15.2	16/20	[39]
rGO/NiO NP with SnO$_2$ nanoplates	NO$_2$	Room temperature	60 (5–60)	$G_g - G_o/G_o$ = 62.28	220/835	[82]
rGO/CuO nanohybrid	NO$_2$	135 (25–225)	75 (1–75)	$I_{gas} - I_{air}/I_{air}$ = 51.7	50/105	[83]
rGO/CuFe$_2$O$_4$ nanoparticles	NH$_3$	110	200 (5–200)	$R_g - R_a/R_a$ = 24.41	3/6	[50]
rGO/Fe$_3$O$_4$ nanoparticles	Ethanol	Room temperature	1	$R_{air} - R_{gas}/R_{gas}$ = 1.86	—	[48]
	NO$_2$	200 (250–450)	2.5 (1–5)	$R_{air} - R_{gas}/R_{gas}$ = 4.68	—	
Graphene/WO$_3$ nanoparticle	NO$_2$	250 (200–300)	5 (1–20)	R_{gas}/R_{air} = 133	~25/—	[84]
Graphene-CeO$_2$ nanoparticles	NO$_2$	—	(10–200 ppm)	—	—	[85]

Table 1.
Summary of the performance of sensors fabricated by using the nanocomposites of metal oxide nanoparticles (0-D) and graphene or graphene derivatives (GO, rGO).

nanoparticles like NiO, CuO, WO$_3$, Fe$_3$O$_4$, CeO$_2$, etc. were reported as promising gas/vapor sensing composite materials with graphene and its derivatives. However, among all the target gases and vapors, NO$_2$ was the mostly explored gas and detected successfully by graphene/metal oxide nanocomposite sensors [79]. Other gases like H$_2$, NH$_3$, CO, C$_2$H$_2$, CH$_4$, SO$_2$, and organic vapors like acetone, ethanol,

methanol, and formaldehyde were detected successfully by using graphene/NP metal oxide hybrids. Sensors were tested at different temperature range varying from room temperature ~25°C to 400°C. The average operating temperature of graphene/NP metal oxide nanocomposites was recorded below 150°C. Among the 37 research articles, room temperature sensing was reported by 13 groups of researchers mentioned in the literature. The detailed transient behavior of graphene/metal oxide NPs sensors is shown in **Figure 11(a–f)** where all the sensing was reported at room temperature. So, overall study confirms the lowering of gas sensing the temperature of metal oxide nanoparticles due to the formation of composites with graphene, GO, and rGO. Most of the article showed a lower detection limit of gases and vapors (<100 ppm). Depending on the surface morphology, sensing temperature and device structures the detection range varied from ppb to ppm level as shown in **Table 1**. Finally, the response magnitude and response/recovery time were fully dependent on the operating temperature and concentration range of the analyte. However, all the sensors showed adequate response magnitude towards the target gas/vapors. Response/recovery time increased and decreased with decrease and increase of operating temperature, respectively. Response time and recovery time varied from 1 s to 220 s and 1 s to 1552 s, respectively, as shown in **Table 1**. Wang et al. confirmed that the uniform distribution of SnO_2 nanoparticles on rGO sheets is an effective factor for enhanced NO_2 sensing performances [42]. The p-n junction existed in the interface of nanoparticle and rGO contributed to good room temperature NO_2 sensing properties which is associated with the valid electron flow from SnO_2 nanoparticle to rGO.

3.2 Sensing performance of graphene/1-D metal oxides composites

One dimensional (1-D) metal oxide like nanorods, nanotubes, nanowires, nanofibers, quantum nanowires, etc. functionalized by graphene, GO, and rGO
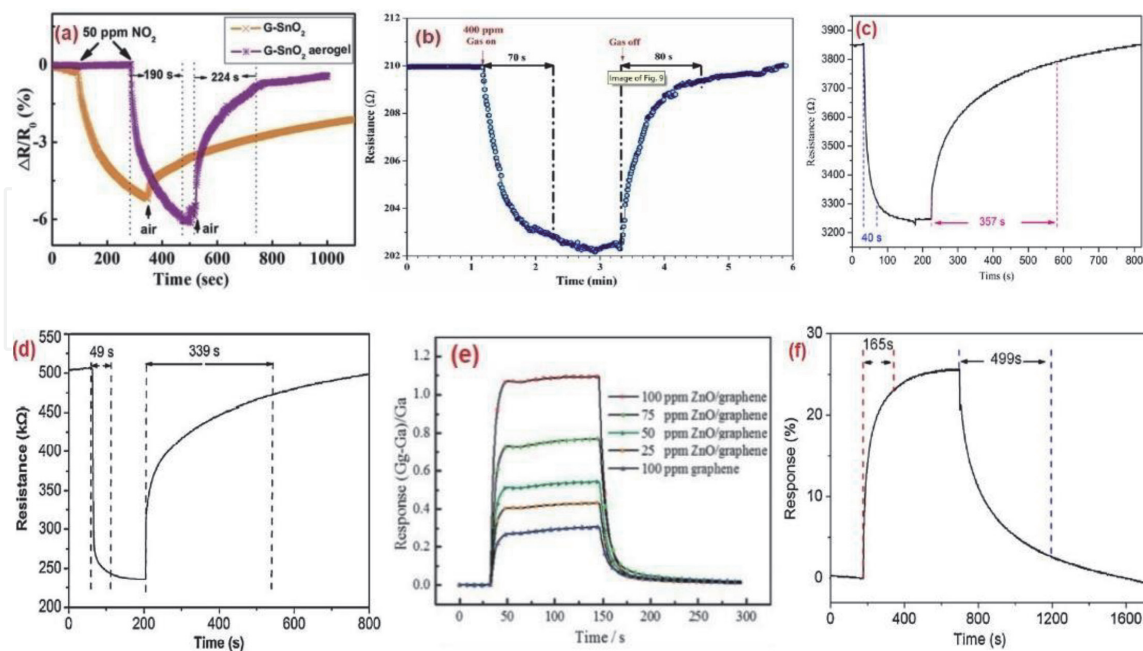

Figure 11.
Room temperature sensing of graphene (GO, rGO)/metal oxide nanoparticles composites. (a) NO_2 sensing by graphene aerogel/SnO_2 nanoparticle [71], (b) CO sensing by rGO/SnO_2 nanoparticles [76], (c) NO_2 sensing by sulfonated graphene/SnO_2 nanoparticles [77], (d) NO_2 sensing by rGO/SnO_2 nanoparticles with Ag NPs [78], (e) formaldehyde sensing by graphene-ZnO quantum dots [46], and (f) NO_2 sensing by rGO/ZnO nanoparticles [80].

Composite material	Target gas/ vapor	Operating temperature (range) (°C)	Concentration and range (ppm)	Response magnitude	Response/ recovery time (s)	Ref.
rGO/ZnO nanorods	NO_2	Room temperature	1 (0.120–1)	$R_{gas} - R_{air}/R_{air}$ = 50%	120/320	[86]
Functionalized graphene/ZnO nanorods	Ethanol	340 (200–370)	100	$R_{air} - R_{gas}/R_{air}$ = 93.5%	5/20	[28]
rGO/ZnO nanofibers	NO_2	400 (300–400)	5 (1–5)	R_{gas}/R_{air} = 119	143/259	[54]
	CO	400 (300–400)	5 (1–5)	R_{air}/R_{gas} = 22.6	—	
Non-oxidized graphene/ZnO nanofibers	Acetone	350 (250–450)	5 (1–5)	R_{air}/R_{gas} = 18.5	12.8/—	[59]
rGO/ZnO nanotubes	Ethanol	125 (27–150)	100 (1–800)	79.14%	41.1/98.32	[63]
rGO/ZnO nanorods	Ethanol	260	50 (5–50)	R_{air}/R_{gas} = ~27	<10/<10	[30]
rGO/ZnO nanorods	NO_2	Room temperature	1 (1–10)	$R_{air} - R_{gas}/R_{gas}$ = 1.19	75/132	[29]
Graphene/ZnO nanorod doped by Au/Ti	Ethanol	300	50 (10–50)	R_{air}/R_{gas} = ~90	—	[55]
Au/Pd functionalized rGO/ZnO nanofiber	CO	400 (300–450)	5 (1–5)	R_{air}/R_{gas} = 35.8	191.3/82.1	[87]
	C_6H_6	400 (300–450)	5 (1–5)	R_{air}/R_{gas} = 22.8	110.3/318.2	
rGO/SnO_2 nanofibers	H_2S	200	5 (1–5)	R_{air}/R_{gas} = 33.7	<198/<114	[53]
	Acetone	350 (150–400)	5 (1–5)	R_{air}/R_{gas} = 10.4	<198/<114	
Graphene/SnO_2 nanowires	NO_2	150 (100–250)	0.1 (0.01–0.1)	R_{air}/R_{gas} = 11	43/37	[26]
Graphene/SnO_2 nanorods	H_2S	260	50 (1–50)	R_{air}/R_{gas} = 130	5/10	[27]
rGO/SnO_2 quantum wires	H_2S	Room temperature	50 (10–100)	R_{air}/R_{gas} = 33	2/292	[25]
Nanoporous graphene hybrid-SnO_2 nanorods	CH_4	150 (100–200)	1000	$|R_{gas} - R_{air}|/R_{air}$ = 24.9 %	369/519.8217.9/242	[88]
rGO/TiO_2 nanotubes	H_2	200 (100–300)	480 (120–480)	$|G_{gas} - G_o|/G_o$ = 37.6	1110/<300	[60]
rGO/TiO_2 nanotubes	Methanol	Room temperature	800 (10–800)	$R_{air} - R_{gas}/R_{air}$ = 96.93%	18/61	[61]
GO/Co_3O_4 nanofibers	Acetone	300 (200–350)	5 (1–5)	R_{gas}/R_{air} = 2.29	—	[58]
rGO/Co_3O_4 nanowires	NH_3	Room temperature	50 (5–100)	$\Delta R/R_{air}$ = 53.6%	4/300	[57]

Composite material	Target gas/ vapor	Operating temperature (range) (°C)	Concentration and range (ppm)	Response magnitude	Response/ recovery time (s)	Ref.
rGO/Cu$_2$O nanowires	NO$_2$	Room temperature	2 (0.4–2)	I$_{gas}$ − I$_{air}$/I$_{air}$ = 67.8%	—	[89]
Graphene/WO$_3$ nanorods	NO$_2$	300	20 (0.025–20)	R$_{gas}$/R$_{air}$ = 202	—	[56]
rGO/αFe$_2$O$_3$ nanofibers	Acetone	375 (250–400)	100 (0.05–2)	R$_{air}$/R$_{gas}$ = 8.9	3/9	[18]

Table 2.
Summary of the performance of the sensor fabricated by using the nanocomposites of 1-D metal oxides and graphene or graphene derivatives (GO, rGO).
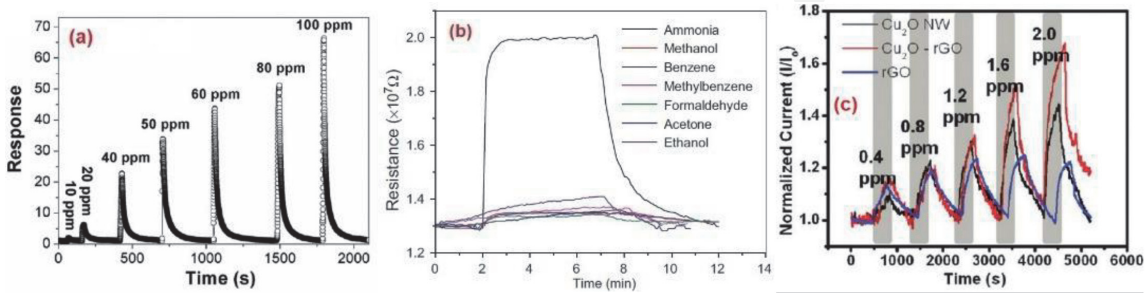

Figure 12.
Room temperature transient response of graphene/1-D metal oxide nanocomposites sensors. (a) H$_2$S detection by for rGO/SnO$_2$ quantum wires [25], (b) selective NH$_3$ sensing by rGO/Co$_3$O$_4$ nanowires [57], and (c) NO$_2$ sensing was observed for rGO/Cu$_2$O nanowires [89].

were reported as the promising gas sensing materials. A total of 21 reports on graphene/1-D metal oxide nanocomposites have been summarized in **Table 2** and compared in terms of target gas/vapors and its concentration, operating temperature, response magnitude, and response/recovery time. In the case of 1-D nanomaterials, ZnO was most explored metal oxide used to synthesize nanocomposites with rGO in the form of nanorods, nanotubes, and nanofibers. Other metal oxides are SnO$_2$ nanofibers/nanorods, TiO$_2$ nanotubes, Co$_3$O$_4$ nanofibers, WO$_3$nanorods, αFe$_2$O$_3$ nanofibers, etc. reported for nanocomposites with graphene for gas sensing application. NO$_2$ and ethanol were the mostly explored target gas and vapor in case of graphene/1-D metal oxide nanocomposites. Other selective gases and vapors are CO, H$_2$S, CH$_4$, H$_2$, NH$_3$, acetone, benzene, methanol, etc. Though the operating temperature range was in-between room temperature ~25°C and 450°C, average sensing temperature was slightly high (~200°C) in case of 1-D compared with 0-D metal oxide nanocomposites with graphene. However, the detection range of gases/vapors was quite small in case of graphene/1-D metal oxide nanocomposites where 1 ppm and below 1 ppm detection were reported frequently. Quite a high response magnitude and moderate response/recovery time were recorded in case of graphene/1-D metal oxide nanocomposites.

Figure 12(a) represents very efficient H$_2$S sensing for rGO/SnO$_2$ quantum wires sensor for the concentration range of 10–100 ppm at room temperature. Being a room temperature sensing, the sensor showed a very fast response of 2 s only [25]. Highly selective NH$_3$ sensing was reported for rGO/Co$_3$O$_4$ nanowires at room temperature as shown in **Figure 12(b)** where response time was only 4 s [57]. Improvised NO$_2$ sensing was observed for rGO/Cu$_2$O nanowires compared with the pure Cu$_2$O nanowires and pure rGO in the concentration range of 0.4–2 ppm at room temperature (**Figure 12(c)**) [89]. However, the overall study envisages the potential gas sensing of 1-D metal oxides functionalized by graphene, GO, and rGO.

The 1-dimensional structure of TiO_2 nanotubes (NTs) in its hybrid with rGO provided large amount of gas interaction sites which lead to high response magnitude of the sensor [61].

3.3 Sensing performance of graphene/2-D metal oxides composites

Table 3 shows gas sensing performance of 2-D metal oxides and GO (or rGO) nanocomposites where ZnO, SnO_2, and WO_3 nanosheets were used as 2-D materials. Relatively high operating temperature was reported for graphene/2-D metal oxide nano composites. Average sensing temperature was more than 200°C. Moderate response magnitude, response/recovery time were recorded for graphene/2-D metal oxide nano composites. Transient behavior of GO/ZnO nanosheets in the exposure of 100 ppm acetone at 240°C and rGO/hexagonal WO_3nanosheets in the exposure of 40 ppm H_2S at 350°C are shown in **Figure 13(a)** and **(b)** [66, 67].

3.4 Sensing performance of graphene/2-D metal oxides composites

The gas sensing performance of nanocomposites developed by 3-D metal oxide and graphene derivatives are shown in **Table 4**. Nanoflowers and nanosphere structures were reported here. Interestingly, all the nanocomposites showed their

Composite material	Target gas/ vapor	Operating temperature (range) (°C)	Concentration and range (ppm)	Response magnitude	Response/ recovery time (s)	Ref.
rGO/Ni-doped ZnO nanoplates	H_2	150	100 (1–100)	$\lvert R_{air} - R_{gas}\rvert/ R_{air} = 63.8\%$	28/—	[64]
GO/ZnO nanosheets	Acetone	240	100 (50–500)	$R_{air}/R_{gas} = 35.8\%$	13/7	[66]
rGO nanosheets/ wrinkled SnO_2	Ethanol	250 (150–300)	100 (5–5000)	$R_{air}/R_{gas} = 80\%$	9/457	[65]
rGO/hexagonal WO_3 nanosheets	H_2S	350 (50–400)	40 (0.01–40)	$\lvert R_{gas} - R_{air}\rvert/ R_{air} = 168.58\%$	7/55	[67]

Table 3.
Summary of the performance of a sensor fabricated by using the nanocomposites of 2-D metal oxides and graphene or graphene derivatives (GO, rGO).
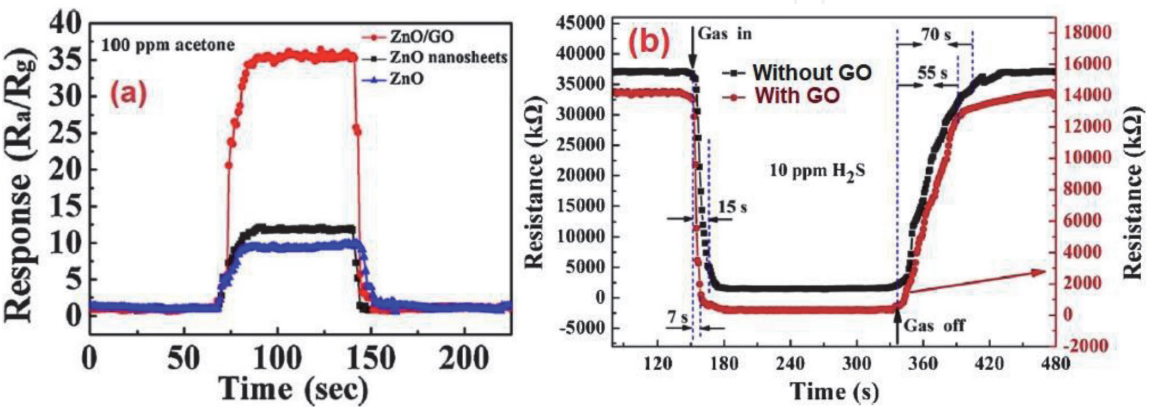

Figure 13.
Response behavior of (a) GO/ZnOnanosheets in the exposure of 100 ppm acetone at 240°C [66] and (b) rGO/hexagonal WO_3nanosheets in the exposure of 40 ppm H_2S at 350°C [67].

Composite material	Target gas/ vapor	Operating temperature (range) (°C)	Concentration and range (ppm)	Response magnitude	Response/ recovery time (s)	Ref.
rGO/ZnO nanoflower	NO_2	100 (50–150)	0.5 (0.005–0.5)	R_{gas}/R_{air} = 12	258/288	[15]
rGO/In$_2$O$_3$ nanoflower	NO_2	74 (25–110)	1 (0.01–1)	R_{gas}/R_{air} = 1337	208/39	[68]
rGO/Fe$_2$O$_3$ nanosphere	NO_2	Room temperature	90 (0.18–90)	$R_{air} - R_{gas}/R_{gas}$ = 150.63%	80/1648	[69]
rGO/CuO nanoflower	NO_2	Room temperature	1000 (0.25–1000)	$|R_{gas} - R_{air}|/R_{air}$ = 6.61 %	76/232	[90]
Graphene/ WO$_3$ nanosphere	NO_2	Room temperature	56 (7–56)	$I_{gas} - I_{air}/I_{air}$ = 40.8%	—	[70]
rGO/WO$_3$ porous nanoflakes	NO_2	90 (20–200)	10 (5–200)	R_{gas}/R_{air} = 5%	4.1/5.8	[91]

Table 4.
Summary of the performance of sensor fabricated by using the nanocomposites of 3-D metal oxides and graphene or graphene derivatives (GO, rGO).
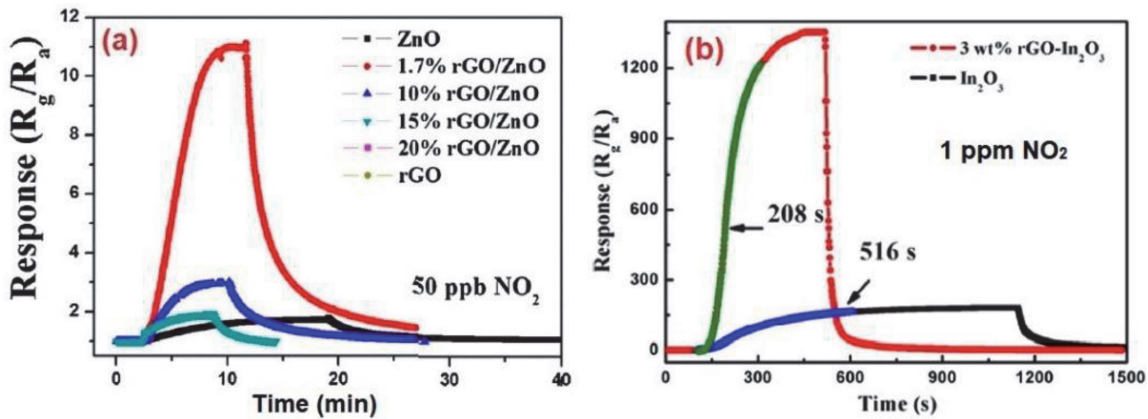

Figure 14.
NO$_2$ response of (a) rGO/ZnO nanoflower (1.7% rGO in ZnO) at 100°C [15] and (b) rGO/In$_2$O$_3$nanoflower at 74°C [68].

selective behavior towards NO_2. Operating temperature of the sensor was quite low and most of the cases room temperature sensing was reported. The detection range was quite high where lower and higher detection limit varied from a few ppb to 1000 ppm. Very high response magnitude was reported in case of graphene/3-D metal oxide nanocomposites. Reported response time and recovery time were quite high in the case of 3-D metal oxide composites compared with 0-D and 1-D metal oxide nanocomposites. Highly selective NO_2 sensing was reported for rGO/ZnO nanoflower (1.7% rGO in ZnO) as shown in **Figure 14(a)**. Promising NO_2 sensing was observed for rGO/In$_2$O$_3$ nanoflower where the response was poor for pure In$_2$O$_3$nanoflower as shown in **Figure 14(b)**. The nanoflower-shaped CuO nano-structure in its nanocomposite with rGO is effective to prevent the aggregation of rGO sheets and form porous structure with rGO, which greatly facilitate the adsorption and diffusion of gas molecules [92].

4. Conclusion

Hybrids of graphene/nanoscale metal oxides have been extensively discussed in this chapter where the major focused area was synthesis/fabrication of monohybrid and its performance assessment for gas/vapor sensing applications. Detailed literature survey confirmed that metal oxide nanoparticle (0-D) are the most reported nanostructure used for the synthesis of nanocomposites with graphene (and GO and rGO) for potential gas sensing application while 1-D metal oxides like nanorods, nanotubes, nanowires, etc. were in the second place. Use of 2-D and 3-D metal oxides were relatively less to form composites with graphene. In chemical synthesis, GO/rGO functionalization was carried out in two routes, that is, (i) mixing of GO/rGO in precursor before synthesizing a nanostructure and (ii) functionalization by GO/rGO after synthesis of nanostructures. Hydrothermal was the most popular method followed by solvothermal, sol-gel, spray pyrolysis, etc. reported to synthesize a composite of 0-D metal oxides. Hydrothermal, electrospinning, electrochemical anodization, etc. were used for the synthesis of graphene/1-D metal oxide composites. Most of the 2-D and 3-D nanocomposites were grown by low-cost chemical methods. Therefore, the graphene/nanoscale metal oxide composites can synthesize via a cost-effective way.

Among all the metal oxides, SnO_2 was mostly reported materials in 0-D structure used in composites with graphene. Other popular metal oxides are ZnO, WO_3 and TiO_2 mostly used for 1-D metal oxide hybrid. A large number of the report showed NO_2 selective behavior of rGO/metal oxide nanocomposite gas sensors especially for 3-D and 0-D metal oxide hybrids. Other reported gases/vapors are H_2, NH_3, CO, H_2S, C_2H_2, ethanol, methanol, acetone, benzene, etc. A significant variation was observed in case of operating temperature of the sensors in case of different nanoscale metal oxides. The average sensing temperature was highest in case of 2-D nanocomposites and decreased from 1-D, 0-D and 3-D. However, the overall study confirmed the relatively low-temperature detection of gases and vapors after the formation of composites of graphene and nanoscale metal oxides. The detection range was varying from lower ppb to higher ppm level but most of the report was confined near a low ppm range (1–100 ppm). A significant improvement was also observed in case of response magnitude and response time/recovery time.

Finally, we would like to conclude with the comment that gas/vapor sensing performance was improved significantly due to the formation of nanohybrid of nanoscale metal oxides and graphene derivatives like GO and rGO. Further study may be necessary with these nano thin-film sensors to encourage the performance in terms of high selectivity and long-term stability. Then these hybrid sensors to make these nanocomposite sensors more suitable for practical applications.

Acknowledgements

Author details

Arnab Hazra[1*], Nagesh Samane[1] and Sukumar Basu[2]

1 Department of Electrical and Electronics Engineering, Birla Institute of Technology and Science (BITS)-Pilani, VidyaVihar, Rajasthan, India

2 Department of Physics and Materials Science, Jaypee University of Information Technology (JUIT), Solan, India

*Address all correspondence to: arnab.hazra@pilani.bits-pilani.ac.in

IntechOpen

References

[1] Hosseini MS, Zeinali S, Sheikhi MH. Fabrication of capacitive sensor based on Cu-BTC (MOF-199) nanoporous film for detection of ethanol and methanol vapors. Sensors and Actuators B: Chemical. 2016;**230**:9-16. DOI: 10.1016/j.snb.2016.02.008

[2] Righettoni M, Amann A, Pratsinis SE. Breath analysis by nanostructured metal oxides as chemo-resistive gas sensors. Materials Today. 2015;**18**:163-171. DOI: 10.1016/j.mattod.2014.08.017

[3] Fratoddi I, Bearzotti A, Venditti I, Cametti C, Russo MV. Role of nanostructured polymers on the improvement of electrical response-based relative humidity sensors. Sensors and Actuators B: Chemical. 2016;**225**:96-108. DOI: 10.1016/j.snb.2015.11.001

[4] Gupta CS, Chatterjee S, Ray AK, Chakraborty AK. Graphene-metal oxide nanohybrids for toxic gas sensor: A review. Sensors and Actuators B. 2015;**221**:1170-1181. DOI: 10.1016/j.snb.2015.07.070

[5] Bindra P, Hazra A. Impedance behavior of n-type TiO_2 nanotubes porous layer in reducing vapor ambient. Vacuum. 2018;**152**:78-83. DOI: 10.1016/j.vacuum.2018.03.008

[6] Tang X, Mager N, Vanhorenbeke B, Hermans S, Raskin J-P. Defect-free functionalized graphene sensor for formaldehyde detection. Nanotechnology. 2017;**28**:055501. DOI: 10.1088/1361-6528/28/5/055501

[7] Hazra A, Dutta K, Bhowmik B, Manjuladevi V, Gupta RK, Bhattacharyya P. Low temperature methanol sensing by p-type nano-titania: Correlation with defects states and Schottky barrier model. IEEE Transactions on Nanotechnology. 2015;**14**:187-195. DOI: 10.1109/TNANO.2014.2376633

[8] Hazra A, Dutta K, Bhowmik B, Bhattacharyya P. Highly repeatable low-ppm ethanol sensing characteristics of p-TiO_2-based resistive devices. IEEE Sensors Journal. 2014;**15**:408-416. DOI: 10.1109/JSEN.2014.2345575

[9] Bindra P, Hazra A. Capacitive gas and vapor sensors using nanomaterials. Journal of Materials Science: Materials in Electronics. 2018;**29**:6129-6148. DOI: 10.1007/s10854-018-8606-2

[10] Liu X, Chang S, Liu H, Hu S, Zhang D, Ning H. A survey on gas sensing technology. Sensors. 2012;**12**:9635-9665. DOI: 10.3390/s120709635

[11] Jiménez-Cadena G, Riu J, Riusa FX. Gas sensors based on nanostructured materials. The Analyst. 2007;**132**:1083-1099. DOI: 10.1039/b704562j

[12] Singh E, Meyyappan M, Nalwa HS. Flexible graphene-based wearable gas and chemical sensors. ACS Applied Materials & Interfaces. 2017;**9**:34544-34586. DOI: 10.1021/acsami.7b07063

[13] Wang Y, Zhang L, Hu N, Wang Y, Zhang Y, Zhou Z, et al. Ammonia gas sensors based on chemically reduced graphene oxide sheets self-assembled on Au electrodes. Nanoscale Research Letters. 2014;**9**:251. DOI: 10.1186/1556-276X-9-251

[14] Lu G, Ocola LE, Chen J. Reduced graphene oxide for room-temperature gas sensors. Nanotechnology. 2009;**20**:445502. DOI: 10.1088/0957-4484/20/44/445502

[15] Liu J, Li S, Zhang B, Xiao Y, Gao Y, Yang Q, et al. Ultrasensitive and low detection limit of nitrogen dioxide gas sensor based on flower-like ZnO hierarchical nanostructure modified by reduced graphene oxide. Sensors and

Actuators B. 2017;**249**:715-724. DOI: 10.1016/j.snb.2017.04.190

[16] Venkatesan A, Rathi S, Lee I-Y, Park J, Lim D, Kim G-H, et al. Low temperature hydrogen sensing using reduced graphene oxide and tin oxide nanoflowers based hybrid structure. Semiconductor Science and Technology. 2016;**31**:125014. DOI: 10.1088/0268-1242/31/12/125014

[17] Cui S, Pu H, Lu G, Wen Z, Mattson EC, Hirschmugl C, et al. Fast and selective room-temperature ammonia sensors using silver nanocrystal-functionalized carbon nanotubes. ACS Applied Materials & Interfaces. 2012;**4**:4898-4904. DOI: 10.1021/am301229w

[18] Guo L, Kou X, Dinga M, Wanga C, Dong L, Zhang H, et al. Reduced graphene oxide/α-Fe_2O_3 composite nanofibers for application in gas sensors. Sensors and Actuators B. 2017;**244**:233-242. DOI: 10.1016/j.snb.2016.12.137

[19] Inyawilert K, Wisitsoraat A, Sriprachaubwong C, Tuantranont A, Phanichphant S, Liewhiran C. Rapid ethanol sensor based on electrolytically-exfoliated graphene-loaded flame-made In-doped SnO_2 composite film. Sensors and Actuators B. 2015;**209**:40-55. DOI: 10.1016/j.snb.2014.11.086

[20] Xiao Y, Yang Q, Wang Z, Zhang R, Gao Y, Sun P, et al. Improvement of NO_2 gas sensing performance based on discoid tin oxide modified by reduced graphene oxide. Sensors and Actuators B. 2016;**227**:419-426. DOI: 10.1016/j.snb.2015.11.051

[21] Rao CNR, Sood AK, Subrahmanyam KS, Govindaraj A. Graphene: The new two-dimensional nanomaterial. Angewandte Chemie, International Edition. 2009;**48**:7752-7777. DOI: 10.1002/anie.200901678

[22] Randviir EP, Brownson DAC, Banks CE. A decade of graphene research: Production, applications and outlook. Materials Today. 2014;**17**:426-432. DOI: 10.1016/j.mattod.2014.06.001

[23] Edwards RS, Coleman KS. Graphene synthesis: Relationship to applications. Nanoscale. 2013;**5**:38-51. DOI: 10.1039/C2NR32629A

[24] Mohan VB, Lau K-T, Hui D, Bhattacharyya D. Graphene-based materials and their composites: A review on production applications and product limitations. Composites Part B Engineering. 2018;**142**:200-220. DOI: 10.1016/j.compositesb.2018.01.013

[25] Song Z, Wei Z, Wang B, Luo Z, Xu S, Zhang W, et al. Sensitive room-temperature H_2S gas sensors employing SnO_2 quantum wire/reduced graphene oxide nanocomposites. Chemistry of Materials. 2016;**28**:1205-1212. DOI: 10.1021/acs.chemmater.5b04850

[26] Quang VV, Dung NV, Trong NS, Hoa ND, Duy NV, Hieu NV. Outstanding gas-sensing performance of graphene/SnO_2 nanowire Schottky junctions. Applied Physics Letters. 2014;**105**:1-5. DOI: 10.1063/1.4887486

[27] Zhang Z, Zou R, Song G, Yu L, Chen Z, Hu J. Highly aligned SnO_2 nanorods on graphene sheets for gas sensors. Journal of Materials Chemistry. 2011;**21**:17360-17365. DOI: 10.1039/c1jm12987b

[28] Song N, Fan H, Tian H. PVP assisted in situ synthesis of functionalized graphene/ZnO (FGZnO) nanohybrids with enhanced gas-sensing property. Journal of Materials Science. 2015;**50**:2229-2238. DOI: 10.1007/s10853-014-8785-z

[29] Xia Y, Wang J, Xu JL, Li X, Xie D, Xiang L, et al. Confined formation of ultrathin ZnO nanorods/reduced graphene oxide mesoporous

nanocomposites for high-performance room-temperature NO_2 sensors. ACS Applied Materials & Interfaces. 2016;**8**: 35454-35463. DOI: 10.1021/acsami. 6b12501

[30] Zou R, He G, Xu K, Liu Q, Zhang Z, Hu J. ZnO nanorods on reduced graphene sheets with excellent field emission, gas sensor and photocatalytic properties. Journal of Materials Chemistry A. 2013;**1**:8445-8452. DOI: 10.1039/c3ta11490b

[31] Dhall S, Kumar M, Bhatnagar M, Mehta BR. Dual gas sensing properties of graphene-Pd/SnO_2 composites for H_2 and ethanol: Role of nanoparticles-graphene interface. International Journal of Hydrogen Energy. 2018;**43**: 17921-17927. DOI: 10.1016/j. ijhydene.2018.07.066

[32] Singkammo S, Wisitsoraat A, Sriprachuabwong C, Tauntranout A, Phanichphat S, Liewhiran C. Electrolytically exfoliated graphene-loaded flame-made Ni-doped SnO_2 composite film for acetone sensing. ACS Applied Materials & Interfaces. 2015;**7**: 3077-3092. DOI: 10.1021/acsami. 5b00161

[33] Zhang D, Liu A, Chang H, Xia B. Room-temperature high-performance acetone gas sensor based on hydrothermal synthesized SnO_2-reduced graphene oxide hybrid composite. RSC Advances. 2015;**5**: 3016-3022. DOI: 10.1039/C4RA10942B

[34] Zhang H, Wang L, Zhang T. Reduced graphite oxide/SnO_2/Au hybrid nanomaterials for NO_2 sensing performance at relatively low operating temperature. RSC Advances. 2014;**4**: 57436-57441. DOI: 10.1039/ C4RA10474A

[35] Zhang H, Feng J, Fei T, Liu S, Zhang T. SnO_2 nanoparticles-reduced graphene oxide nanocomposites for NO_2 sensing at low operating temperature. Sensors and Actuators B: Chemical.

2014;**190**:472-478. DOI: 10.1016/j. snb.2013.08.067

[36] Mishra RK, Upadhyay SB, Khushwaha A, Kim TH, Murali G, Verma R, et al. SnO_2 quantum dots decorated on RGO: A superior sensitive, selective and reproducible performance for a H_2 and LPG sensor. Nanoscale. 2015;**7**:11971-11979. DOI: 10.1039/ c5nr02837j

[37] Ghosh R, Nayak AK, Santra S, Pradhan D, Guha PK. Enhanced ammonia sensing at room temperature with reduced graphene oxide/tin oxide hybrid films. RSC Advances. 2015;**5**: 50165-50173. DOI: 10.1039/ C5RA06696D

[38] Jin L, Chen W, Zhang H, Xiao G, Yu C, Zhou Q. Characterization of reduced graphene oxide (rGO)-loaded SnO_2 nanocomposite and applications in C_2H_2 gas detection. Applied Sciences. 2016;**7**:19. DOI: 10.3390/app7010019

[39] Zhang D, Chang H, Li P, Liu R. Characterization of nickel oxide decorated-reduced graphene oxide nanocomposite and its sensing properties toward methane gas detection. Journal of Materials Science: Materials in Electronics. 2016;**27**: 3723-3730. DOI: 10.1007/s10854-015-4214-6

[40] Wang Z, Zhang T, Han T, Fei T, Liu S, Lu G. Oxygen vacancy engineering for enhanced sensing performances: A case of SnO_2 nanoparticles-reduced graphene oxide hybrids for ultrasensitive ppb-level room-temperature NO_2 sensing. Sensors and Actuators B: Chemical. 2018;**266**: 812-822. DOI: 10.1016/j.snb.2018.03.169

[41] Peng R, Chen J, Nie X, Li D, Si P, Feng J, et al. Reduced graphene oxide decorated Pt activated SnO_2 nanoparticles for enhancing methanol sensing performance. Journal of Alloys and Compounds. 2018;**762**:8-15. DOI: 10.1016/j.jallcom.2018.05.177

[42] Wang Z, Han T, Fei T, Liu S, Zhang T. Investigation of microstructure effect on NO_2 sensors based on SnO_2 nanoparticles/reduced graphene oxide hybrids. ACS Applied Materials & Interfaces. 2018;**10**: 41773-41783. DOI: 10.1021/ acsami.8b15284

[43] Tammanoon N, Wisitsoraat A, Spriprachuabwong C, Phokharatkul D, Tauntranout A, Phanichphant S, et al. Ultrasensitive NO_2 sensor based on Ohmic metal-semiconductor interfaces of electrolytically exfoliated graphene/flame-spray-made SnO_2 nanoparticles composite operating at low temperatures. ACS Applied Materials & Interfaces. 2015;**7**: 24338-24352. DOI: 10.1021/ acsami.5b09067

[44] Iftekhar Uddin ASM, Phan DT, Chung GS. Low temperature acetylene gas sensor based on Ag nanoparticles-loaded ZnO-reduced graphene oxide hybrid. Sensors and Actuators B: Chemical. 2015;**207**:362-369. DOI: 10.1016/j.snb.2014.10.091

[45] Uddin ASMI, Chung GS. Synthesis of highly dispersed ZnO nanoparticles on graphene surface and their acetylene sensing properties. Sensors and Actuators B: Chemical. 2014;**205**: 338-344. DOI: 10.1016/j.snb.2014. 09.005

[46] Huang Q, Zeng D, Li H, Xie C. Room temperature formaldehyde sensors with enhanced performance, fast response and recovery based on zinc oxide quantum dots/graphene nanocomposites. Nanoscale. 2012;**4**:5651-5658. DOI: 10.1039/ c2nr31131c

[47] Liu S, Wang Z, Zhang Y, Dong Z, Zhang T. Preparation of zinc oxide nanoparticle-reduced graphene oxide-gold nanoparticle hybrids for detection of NO_2. RSC Advances. 2015; **5**:91760-91765. DOI: 10.1039/ c5ra18680c

[48] Tung TT, Chien NV, Duy NV, Hieu NV, Nine MJ, Coghlan CJ, et al. Magnetic iron oxide nanoparticles decorated graphene for chemoresistive gas sensing: The particle size effects. Journal of Colloid and Interface Science. 2019;**539**:315-325. DOI: 10.1016/j. jcis.2018.12.077

[49] Kamal T. High performance NiO decorated graphene as a potential H_2 gas sensor. Journal of Alloys and Compounds. 2017;**729**:1058-1063. DOI: 10.1016/j.jallcom.2017.09.124

[50] Achary LSK, Kumar A, Barik B, Nayak PS, Tripathy N, Kar JP, et al. Reduced graphene oxide-$CuFe_2O_4$ nanocomposite: A highly sensitive room temperature NH_3 gas sensor. Sensors and Actuators B: Chemical. 2018;**272**: 100-109. DOI: 10.1016/j.snb.2018. 05.093

[51] Neri G, Leonardi SG, Latino M, Donato N, Baek S, Conte DE, et al. Sensing behavior of SnO_2/reduced graphene oxide nanocomposites toward NO_2. Sensors and Actuators B: Chemical. 2013;**179**:61-68. DOI: 10.1016/j.snb.2012.10.031

[52] Kim HW, Na HG, Kwon YJ, Kang SY, Choi MS, Bang JH, et al. Microwave-assisted synthesis of graphene-SnO_2 nanocomposites and their applications in gas sensors. ACS Applied Nano Materials. 2017;**9**: 31667-31682. DOI: 10.1021/ acsami.7b02533

[53] Choi SJ, Jong BH, Lee SJ, Min BK, Rothschild A, Kim ID. Selective detection of acetone and hydrogen sulfide for the diagnosis of diabetes and halitosis using SnO_2 nanofibers functionalized with reduced graphene oxide nanosheets. ACS Applied Materials & Interfaces. 2014;**6**: 2588-2597. DOI: 10.1021/am405088q

[54] Abideen ZU, Katoch A, Kim JH, Kwon YJ, Kim HW, Kim SS. Excellent gas detection of ZnO nanofibers by

loading with reduced graphene oxide nanosheets. Sensors and Actuators B: Chemical. 2015;**221**:1499-1507. DOI: 10.1016/j.snb.2015.07.120

[55] Yi J, Lee JM, Park WI. Vertically aligned ZnO nanorods and graphene hybrid architectures for high-sensitive flexible gas sensors. Sensors and Actuators B: Chemical. 2011;**155**: 264-269. DOI: 10.1016/j.snb.2010. 12.033

[56] An X, Yu JC, Hu Y, Yu X, Zhang G. WO_3 nanorods/graphene nanocomposites for high-efficiency visible-light-driven photocatalysis and NO_2 gas sensing. Journal of Materials Chemistry. 2012;**22**:8525-8531. DOI: 10.1039/C2JM16709C

[57] Feng Q, Li X, Wang J, Gaskov AM. Reduced graphene oxide (rGO) encapsulated Co_3O_4 composite nanofibers for highly selective ammonia sensors. Sensors and Actuators B: Chemical. 2016;**222**:864-870. DOI: 10.1016/j.snb.2015.09.021

[58] Choi SJ, Ryu WH, Kim SJ, Cho HJ, Kim ID. Bi-functional co-sensitization of graphene oxide sheets and Ir nanoparticles on p-type Co_3O_4 nanofibers for selective acetone detection. Journal of Materials Chemistry 2014;**2**:7160-7167. DOI: 10.1039/C4TB00767K

[59] Choi SJ, Choi C, Kim SJ, Cho HJ, Jeon S, Kim ID. Facile synthesis of hierarchical porous WO_3 nanofibers having 1D nanoneedles and their functionalization with non-oxidized graphene flakes for selective detection of acetone molecules. RSC Advances. 2015;**5**:7584-7588. DOI: 10.1039/C4RA13791D

[60] Galstyan V, Ponzoni A, Kholmanov I, Natile MM, Comini E, Nematov S, et al. Reduced graphene oxide–TiO_2 nanotube composite: Comprehensive study for gas-sensing applications. ACS Applied Nano Materials. 2018;**1**:7098-7105. DOI: 10.1021/acsanm.8b01924

[61] Acharyya D, Bhattacharyya P. Highly efficient room-temperature gas sensor based on TiO_2 nanotube-reduced graphene-oxide hybrid device. IEEE Electron Device Letters. 2016;**37**: 656-659. DOI: 10.1109/LED.2016. 2544954

[62] Gakhar T, Hazra A. Synthesis of GO loaded TiO_2 nanotubes array by anodic oxidation for efficient detection of organic vapor. Journal of Electronic Materials. 2019;**48**:5342-5347. DOI: 10.1007/s11664-019-07347-8

[63] Maity I, Acharyya D, Huang K, Chung P, Ho M, Bhattacharya P. A comparative study on performance improvement of ZnO nanotubes based alcohol sensor devices by Pd and rGO hybridization. IEEE Transactions on Electron Devices. 2018;**65**:3528-3534. DOI: 10.1109/TED.2018.2846784

[64] Bhati VS, Ranwa S, Rajamani S, Kumari K, Raliya R, Biswas P, et al. Improved sensitivity with low limit of detection of a hydrogen gas sensor based on rGO-loaded Ni-doped ZnO nanostructures. ACS Applied Materials & Interfaces. 2018;**10**:11116-11124. DOI: 10.1021/acsami.7b17877

[65] Zhao C, Gong H, Lan W, Ramachandran R, Xu H, Liu S, et al. Facile synthesis of SnO_2 hierarchical porous nanosheets from graphene oxide sacrificial scaffolds for high-performance gas sensors. Sensors and Actuators B: Chemical. 2018;**258**: 492-500. DOI: 10.1016/j.snb.2017.11.167

[66] Wang P, Wang D, Zhang M, Zhu Y, Xu Y, Ma X, et al. ZnO nanosheets/graphene oxide nanocomposites for highly effective acetone vapor detection. Sensors and Actuators B: Chemical. 2016;**230**:477-484. DOI: 10.1016/j.snb.2016.02.056

[67] Shi J, Cheng Z, Gao L, Zhang Y, Xu J, Zhao H. Facile synthesis of

reduced graphene oxide/hexagonal WO_3 nanosheets composites with enhanced H_2S sensing properties. Sensors and Actuators B: Chemical. 2016;**230**:736-745. DOI: 10.1016/j. snb.2016.02.134

[68] Liu J, Li S, Zhang B, Wang Y, Gao Y, Liang X, et al. Flower-like In_2O_3 modified by reduced graphene oxide sheets serving as a highly sensitive gas sensor for trace NO_2 detection. Journal of Colloid and Interface Science. 2017; **504**:206-213. DOI: 10.1016/j.jcis.2017. 05.053

[69] Dong YL, Zhang XF, Cheng XL, Xu YM, Gao S, Zhao H, et al. Highly selective NO_2 sensor at room temperature based on nanocomposites of hierarchical nanosphere-like α-Fe_2O_3 and reduced graphene oxide. RSC Advances. 2014;**4**:57493-57500. DOI: 10.1039/C4RA10136G

[70] Jie X, Zeng D, Zhang J, Xu K, Wu J, Zhu B, et al. Graphene-wrapped WO_3 nanospheres with room-temperature NO_2 sensing induced by interface charge transfer. Sensors and Actuators B: Chemical. 2015;**220**:201-209. DOI: 10.1016/j.snb.2015.05.047

[71] Li L, He S, Liu M, Zhang C, Chen W. Three-dimensional mesoporous graphene aerogel-supported SnO_2 nanocrystals for high-performance NO_2 gas sensing at low temperature. Analytical Chemistry. 2015;**87**: 1638-1645

[72] Zhang Z, Zou X, Xu L, Liao L, Liu W, Ho J, et al. Hydrogen gas sensor based on metal oxide nanoparticles decorated graphene transistor. Nanoscale. 2015;**7**:10078-10084. DOI: 10.1039/C5NR01924A

[73] Tyagi P, Sharma A, Tomar M, Gupta V. A comparative study of RGO-SnO_2 and MWCNT-SnO_2 nanocomposites based SO_2 gas sensors. Sensors and Actuators B: Chemical. 2017;**248**:980-986. DOI: 10.1016/j. snb.2017.02.147

[74] Cui S, Wen Z, Mattson EC, Mao S, Chang J, Weinert M, et al. Indium-doped SnO_2 nanoparticle-graphene nanohybrids: Simple one-pot synthesis and their selective detection of NO_2. Journal of Materials Chemistry A. 2013; **1**:4462-4467. DOI: 10.1039/ C3TA01673K

[75] Zhu X, Guo Y, Ren H, Gao C, Zhou Y. Enhancing the NO_2 gas sensing properties of rGO/SnO_2 nanocomposite films by using microporous substrates. Sensors and Actuators B: Chemical. 2017;**248**:560-570. DOI: 10.1016/j. snb.2017.04.030

[76] Shojaee M, Nasresfahani S, Sheikhi MH. Hydrothermally synthesized Pd-loaded SnO_2/partially reduced graphene oxide nanocomposite for effective detection of carbon monoxide at room temperature. Sensors and Actuators B: Chemical. 2018;**254**:457-467. DOI: 10.1016/j. snb.2017.07.083

[77] Liu S, Wang Z, Zhang Y, Li J, Zhang T. Sulfonated graphene anchored with tin oxide nanoparticles for detection of nitrogen dioxide at room temperature with enhanced sensing performances. Sensors and Actuators B: Chemical. 2016;**228**:134-143. DOI: 10.1016/j.snb.2016.01.023

[78] Wang Z, Zhang Y, Liu S, Zhang T. Preparation of Ag nanoparticles-SnO_2 nanoparticles-reduced graphene oxide hybrids and their application for detection of NO_2 at room temperature. Sensors and Actuators B: Chemical. 2016;**222**:893-903. DOI: 10.1016/j. snb.2015.09.027

[79] Kumar N, Srivastava AK, Patel HS, Gupta BK, Varma GD. Facile synthesis of ZnO-reduced graphene oxide nanocomposites for NO_2 Gas sensing applications. European Journal of Inorganic Chemistry. 2015; **2015**:1912-1923. DOI: 10.1002/ ejic.201403172

[80] Liu S, Yu B, Zhang H, Fei T, Zhang T. Enhancing NO_2 gas sensing performances at room temperature based on reduced graphene oxide-ZnO nanoparticles hybrids. Sensors and Actuators B: Chemical. 2014;**202**: 272-278. DOI: 10.1016/j.snb.2014.05.086

[81] Ha NH, Thinh DD, Huong NT, Phuong NH, Thach PD, Hong HS. Fast response of carbon monoxide gas sensors using a highly porous network of ZnO nanoparticles decorated on 3D reduced graphene oxide. Applied Surface Science. 2018;**434**:1048-1054. DOI: 10.1016/j.apsusc.2017.11.047

[82] Zhang J, Wu J, Wang X, Zeng D, Xie C. Enhancing room-temperature NO_2 sensing properties via forming heterojunction for NiO-rGO composited with SnO_2 nanoplates. Sensors and Actuators B: Chemical. 2017;**243**: 1010-1019. DOI: 10.1016/j.snb.2016. 12.062

[83] Li Z, Liu Y, Guo D, Guo J, Su Y. Room-temperature synthesis of CuO/ reduced graphene oxide nanohybrids for high-performance NO_2 gas sensor. Sensors and Actuators B: Chemical. 2018;**271**:306-310. DOI: 10.1016/j. snb.2018.05.097

[84] Srivastava S, Jain K, Singh VN, Singh S, Vijayan N, Dilwar N, et al. Faster response of NO_2 sensing in graphene–WO_3 nanocomposites. Nanotechnology. 2012;**23**:205501. DOI: 10.1088/0957-4484/23/20/205501

[85] Zhang L, Fang Q, Huang Y, Xu K, Ma F, Chu PK. Facet-engineered CeO_2/ graphene composites for enhanced NO_2 gas-sensing. Journal of Materials Chemistry C. 2017;**5**:6973-6981. DOI: 10.1039/C7TC01523B

[86] Triet NM, Duy LT, Hwang BU, Haneef A, Siddiqui S, Park KH, et al. High-performance Schottky diode gas sensor based on the heterojunction of three-dimensional nanohybrids of reduced graphene oxide-vertical ZnO

nanorods on an AlGaN/GaN layer. ACS Applied Materials & Interfaces. 2017;**9**: 30722-30732. DOI: 10.1021/acsami. 7b06461

[87] Abideen ZU, Kim JH, Mirzaei A, Kim HW, Kim SS. Sensing behavior to ppm-level gases and synergistic sensing mechanism in metal-functionalized rGO-loaded ZnO nanofibers. Sensors and Actuators B: Chemical. 2018;**255**: 1884-1896. DOI: 10.1016/j.snb.2017. 08.210

[88] Kooti M, Keshtkar S, Askarieh M, Rashidi A. Progress toward a novel methane gas sensor based on SnO_2 nanorods-nanoporous graphene hybrid. Sensors and Actuators B: Chemical. 2019;**281**:96-106. DOI: 10.1016/j. snb.2018.10.032

[89] Deng S, Tjoa V, Fan HM, Tan HR, Sayle DC, Olvio M, et al. Reduced graphene oxide conjugated Cu_2O nanowire mesocrystals for high-performance NO_2 gas sensor. Journal of the American Chemical Society. 2012; **134**:4905-4917. DOI: 10.1021/ja211683m

[90] Yang Y, Tian C, Wang J, Sun L, Shi K, Zhou W, et al. Facile synthesis of novel 3D nanoflower-like Cu_xO/ multilayer graphene composites for room temperature NO_x gas sensor application. Nanoscale. 2014;**6**: 7369-7378. DOI: 10.1039/c4nr00196f

[91] Hao Q, Liu T, Liu J, Liu Q, Jing X, Zhang H, et al. Controllable synthesis and enhanced gas sensing properties of a single-crystalline WO_3-rGO porous nanocomposite. RSC Advances. 2017;**7**: 14192-14199. DOI: 10.1039/ C6RA28379A

[92] Zhang D, Jiang C, Liu J, Cao Y. Carbon monoxide gas sensing at room temperature using copper oxide decorated graphene hybrid nanocomposite prepared by layer-by-layer self-assembly. Sensors and Actuators B: Chemical. 2017;**247**: 875-882. DOI: 10.1016/j.snb.2017.03.108